CAPTURE CROSS SECTION OF C^{13} FOR LOW ENERGY PROTONS

Thesis by

Eric John Woodbury

In Partial Fulfillment of the Requirements

for the Degree of

Doctor of Philosophy

California Institute of Technology

Pasadena, California

1951

ACKNOWLEDGMENTS

It is the author's pleasure to acknowledge the constant aid and encouragement given by Professors R. F. Christy, W. A. Fowler, C. C. Lauritsen, and T. Lauritsen. Without their help the project could never have been undertaken. Financially the work was only possible through the aid given by the Office of Naval Research. This group is to be commended for its efficient handling of the very difficult problems that arise in the support of fundamental research.

The author is indebted to many people who in one way or another helped in the work; J. D. Seagrave whose thesis covered many similar problems, J. D. Gow of the University of California for his part in the ion source development, A. V. Tollestrup who helped formulate the original problem and aided materially in the solution of many of the electronic problems, and V. F. Ehrgott who helped in many of the design problems.

Much of the machine shop work was performed by L. Gililland, George Fastle, and J. Hill. Their careful instruction of the author in the art of metal working was indispensible. James Wilson aided in the later electrical work while W. D. Gibbs did much of the electronic procurement.

Finally the formal completion of this thesis would have been impossible except for the typing of Mary Toyoda and the drafting of Jeanne Antz.

ABSTRACT

In order to measure the capture cross section of C^{13} at the lowest possible energy a scintillation detector in conjunction with a high current ion source was developed. Because of heat dissipation problems the ion source was pulsed and suitable electronic circuitry was developed to take advantage of the peak currents available. With this equipment it was found possible to obtain proton currents of one milliampere and a detection efficiency of eight percent.

At 128 kilovolts the capture cross section is,

$$\sigma = 5.0 \pm 1.0 \times 10^{-33} \text{ cm}^2$$

Of the resulting radiation approximately eighty percent is 8 Mev in energy while the remaining is either a two or three step cascade with gamma ray energies between two and four million volts of energy.

In the equation,

$$\sigma = \frac{a}{E} e^{-\frac{b}{E^{\frac{1}{2}}}}$$

$b = 5.96 \text{ Mev}^{\frac{1}{2}}$, and $a = 10^{-2}$ Mev barn.

TABLE OF CONTENTS

INTRODUCTION

The reaction involving protons and the carbon isotope C^{13} is important because of the unusual nature of the compound nucleus, N^{14}, and because of the role it plays in the generation of solar energy. The detailed study of the reaction at energies above five hundred kilovolts has been undertaken by J. D. Seagrave of this laboratory. On the other hand, the author's interest has been to determine the value of the capture cross section for the reaction at the lowest possible proton energy in order to aid in the extrapolation to solar temperatures.

The solution of the experimental problems that arose required the application of some recent developments. Unlike other cross sections measured in this laboratory at low energies, the only detectable reaction product available is gamma radiation (1)(2). Thus, the first problem met is the low detection efficiency for gamma radiation of most counters. The most commonly used counter, the Geiger tube, suffers from this defect. It also operates on a trigger principle which makes it difficult to reduce the interference from the low energy sources of radiation that are always present in a laboratory. In fact these defects lead one author to state that he doubts if the cross section for the reaction can be determined at all (1). This difficulty was resolved through the use of the recently developed scintillation counter. No specific reference need be given for this counter for the reader can pick up almost any current copy of the Physical Review and find one or more articles describing a new development or a new application of this versatile instrument. After some experimenting a counter was developed utilizing a one inch cube of sodium iodide and a type 5819 photomultiplier

tube. These were arranged so as to give a counting efficiency for gamma radiation of about thirty percent. By placing the counter close to the source it was possible to obtain a detection efficiency of eight percent. It is believed that this is an order of magnitude better than can be obtained with Geiger tubes. Furthermore the pulses from this detector are roughly proportional to the energy lost in the crystal by the gamma rays or other particles being counted. Therefore discrimination against soft background radiation and against hard cosmic radiation is possible.

The cross section for this reaction was estimated to be 4×10^{-33} cm^2 at 130 kilovolts bombarding energy and even with the increased detector efficiency obtained through the use of a scintillation counter this was too small to be measured using proton currents of conventional magnitude. Even the beam current of two hundred and fifty microamperes obtained by R. N. Hall was insufficient [3][4]. The solution to this problem came in the development by J. D. Gow of a pulsed ion source capable of peak proton currents of one milliampere [5]. Although the pulsed current is high, the average current is low. Thus one gains nothing unless an electronic arrangement is made to turn the counters on in synchronism with the proton pulse. This difficulty was not expected to be insurmountable. With the counter in the final form used, where two-thirds of the background was removed through the use of high level discrimination as well as low level discrimination, it would be just possible to do the experiment with a continuous source of the type Hall describes. This was not true, however, with the earlier counters used. Also the actual time required to collect the data would be about the same, even with the advanced counter, so no real advantage could be gained. The equality of times is computed on the basis of obtaining the same theoretical statistical weights. Large

corrections for background such as would be required with the continuous source are very unsatisfying, and it also would be impossible to obtain the background in the same manner the pulsed operation allowed, that is, simultaneously.

Finally one meets with the difficulty of obtaining the carbon isotope. In normal carbon the ratio is about one to ninety, and even with the gains already made this factor would be enough to make the experiment impossible. Recently, however, C^{13} in concentrations up to sixty percent has become commercially available.

The discussion to follow will be broken up into parts describing, first, the ion source and accelerator with the associated electronic equipment, then the counter and its calibration, followed finally by the experiment itself and an interpretation of the results.

PART I.

ION SOURCE AND ACCELERATOR

1. The Ion Source. The first problem studied in this experiment was the construction of a high current ion source. In the past there have been many ion sources designed and constructed that are capable of proton currents of one hundred microamperes or less. Recently R. Hall built an ion source utilizing a high frequency electrical discharge confined to a small space, and obtained resolved proton currents of 200 to 300 microamperes (4). There appear in the literature descriptions of ion sources capable of continuous proton currents as high as one milliampere, but investigation invariably reveals that these sources are experimental models with little or no attempt to focus the ion beam.

Late in 1949 J. D. Gow at the Radiation Laboratory of the University of California at Berkeley constructed an ion source making use of the Philips Ion Gauge or P. I. G. principle (5). He obtained proton currents of one to two milliamperes. Since the peak power required by this source was 600 watts, pulsed operation was mandatory. This was satisfactory for the source was part of the injector for a pulsed linear accelerator.

Estimates of the C^{13} cross section at 130 kilovolts indicated a one milliampere proton current would bring the counting rate above the expected background, so it was decided to duplicate the Gow source. It will be advantageous to first explain the P. I. G. principle and the problems met in the source itself before describing the actual manner in which the current to the source was pulsed and how the beam so obtained was accelerated, focussed, and measured.

In Figure 1 the ion source is shown in diagrammatic form. Suppose that there is no plasma in the chamber, then the electric flux will pass

from the cathodes to the anode as shown by the solid lines in Figure 2. If an electron were released from the cathode by some process it would quickly pass to the anode. The hydrogen pressure in this source is low and so the mean collision path is many times the dimensions of the chamber. If the magnetic coil is energized, a magnetic field is formed coaxial with the axis of the discharge chamber. Because of the magnetic forces an electron released at one of the cathodes will now find it much more difficult to reach the anode. Instead it will be accelerated to the plane of symmetry, and then retarded until it just reaches the other cathode. In the actual arc, the electron will lose some energy and fall short of this cathode to repeat the cycle in the opposite direction. It can make many such transits of the chamber before it is lost to the anode, and the path traveled is many mean collision paths in length. Any positive ions formed will drift slowly towards the cathodes and upon reaching them release secondary electrons to continue the process. This is the simplified picture of the operation of the arc. The advantage gained is in the use of low gas pressure, thus cutting down the probability of the hydrogen ions recombining once they are formed. The low gas pressure also results in low gas consumption when conventional outlet channels are used. Alternately one may use larger exit holes for greater output currents, and shorter exit channels to reduce further the chance of the ions recombining. The use of low gas flow also eliminates the differential pumping systems often required with ion sources.

The actual operation of the arc is of course much more complicated than this due to the presence of the arc plasma, and the theory of the process in detail is still incomplete [6][7]. Needless to say, most of the

problems that arise in the actual operation of this type of source come from complications introduced only in the general theory and are perhaps not easily discussed on the basis of a simple picture. Nevertheless, a few of the difficulties appear to have simple explanations and these will be given here.

One of the most troublesome problems was the occurrence of parasitic arcs in the chamber. This effect will be called the Perry effect as Dr. J. E. Perry, Jr. gave to our knowledge the first explanation of the cause of the trouble. In general the magnetic field and the electric field are collinear throughout the chamber. This is shown in Figure 2a. However, it is possible for the field to become distorted as in Figure 2b through the presence of the iron that is ordinarily used to reduce the size of the magnet coil. There may then exist a region in the upper part of the chamber in which the magnetic field and electric field are at right angles. An electron can become trapped in such a region and be confined to move in circles concentric with the axis of the arc in much the same manner as electrons are trapped in magnetrons. This increases the distance traveled by the electron before it reaches the anode and makes a discharge very probable. In Figure 3 is shown the plot of the magnetic flux along the axis of an early model of the ion source. This model was characterized by a strong tendency to arc in the rear portions of the discharge chamber. In Figure 3 is also shown the axial plot obtained in a later model which was much less prone to discharge in this manner. There is some reason to believe that a completely uniform field may lead to the same trouble, for there will again be regions of perpendicular magnetic and electric fields. This view is supported by the more satisfactory operation obtained with short solenoids symmetrically spaced, than with long coils which give more uniform fields.

Another problem met in the development of the source was a short lifetime. Others have reported rather long lifetimes for such sources and here, as in their work, no wear was ordinarily observed after several hours operation, yet the source would not operate in a stable manner after being run for a few hours. This trouble was ultimately traced to two primary causes but was never completely eliminated. First, the material used in the cathodes greatly affects the lifetime. It was found that while magnesium gives a very nice proton yield and a clean arc it lasts only a short time, becoming pitted after an hour of pulsed operation. Various aluminum alloys give somewhat inferior performance and about the same lifetime. The short lifetime of these alloys is probably due to the magnesium in the alloy for when the softest aluminum commercially available is used, type 2-SF, satisfactory operation and fair lifetimes are obtained. Aluminum, beryllium, and magnesium were the only materials considered because they are the only common metals having low work functions. Oxide cathode materials were not considered because they do not seem to stand up well under ion bombardment [6]. The second cause of a short lifetime was found to be a result of the vacuum pump oil. This trouble was in large part removed by trapping continuously with a dry ice acetone mixture at the pump. It was found that the vacuum would gradually improve for a day or two when trapping and it is believed that this was due to the slow removal of oil or water vapor from the walls of the equipment. The pump oil or its products apparently destroy the secondary emitting properties of the cathode surfaces. This view is supported by the cure which is to operate the discharge on air or oxygen for a few minutes. In later models of the source a side tube containing silver oxide was added to the hydrogen feed system, and by heating this tube a convenient flow of oxygen could be

obtained. It was found that flaming the cathodes with an acetylene torch just before assembly to burn off any organic material left on the surface improved the operation [5].

Electrical disturbances of high frequency are often developed by the arc as might be expected. These seem to be detrimental to the operation of the source and are certainly detrimental to the operation of the associated electronic equipment. It was found possible to suppress most of this interference by the addition of a simple RC filter at the arc chamber. These disturbances in the arc are discussed in detail in the article by Bachus [6].

In normal operation the arc parameters are as follows; arc current is one ampere, arc voltage is 350 volts, and the magnetic field is 1000 gauss at the center of the discharge. The color of the arc is a bright red, indicating a high percentage of dissociated hydrogen. This red color, in the author's experience, is usually associated with a good proton component in the beam for any type of ion source. Under these operating conditions, and using the focusing system to be described, it has been possible to obtain proton currents of one milliampere. This output is very sensitive to foreign material in the arc chamber, for example, air due to a leak in the system.

2. Column, Focusing System, and Auxiliary Ion Source Equipment.

Figure 4 gives a drawing of the ion source and focusing system. This assembly was fastened to a three section accelerating column of the type used on the three million volt Van de Graaff generator at the Kellogg Radiation Laboratory of the California Institute of Technology [1]. The column was held against a manifold to which the target section and vacuum

pumps were joined. The pumping system consisted of an eight inch oil pump and a Welch type 1405 mechanical backing pump. As shown in the photograph, Figure 5, corona rings and voltage dividing resistors were added to the column to improve the stability of operation. The voltage for the acceleration of the ions was supplied by a number of transformer rectifier sets. The highest potential the column would withstand without sparking excessively was 135 kilovolts.

The design of the focusing system is simple. A probe is placed so that a relatively strong fringing field is present at the arc exit to provide rapid acceleration of the ions. It has been found that the higher voltages on the probe result in larger proton yields at the target. The probe was operated at twelve kilovolts, the highest voltage at which stable operation was found. When working with a new ion source the probe current was found to be negligible.

The focusing electrode is somewhat misnamed. The actual focusing occurs at the entrance to the accelerating column as described by R. N. Hall [1]. The focal length of the lens formed by the entrance to the accelerating column depends on the energy of the incident ions. This energy can be adjusted by changing the voltage applied to the focusing electrode. The voltage required is about ten kilovolts in this design. The effect of the lens formed by the probe and focusing electrode is negligible at this voltage. However, it is possible in designs of this sort to increase the focusing electrode potential to fifty kilovolts and accomplish the focusing entirely in this gap. Because this decreases the path traveled by the protons while they have low energy it is a very good way to accomplish the focusing. Voltages limitations prevented its use on this accelerator.

The hydrogen system consisted of a pressure tank, and a palladium leak constructed from a thimble of palladium two inches long, one quarter inch in diameter, and with a wall thickness of 0.030 inch. A heater connected to a Powerstat type variable autotransformer surrounded the thimble. By controlling the heater power the gas flow could be regulated.

3. Electronic Equipment and Current Integrator.

A block diagram of the experimental arrangement is shown in Figure 6. Figures 7 through 10 give the detailed circuit diagrams. The reader is referred to a text such as Elmore and Sands for an explanation of the principles involved in the operation of the individual circuit elements [8]. The discussion to be given will be a description of the sequential operation.

The primary pulse generating circuits were located at the grounded end of the accelerator as it was advantageous to have the primary pulse available at the counters for control purposes. Furthermore it was thought it might be possible to minimize the effects of ripple on the accelerating voltage by synchronizing the pulse rate with the sixty cycle line frequency or a submultiple of this frequency.

The primary pulse is generated by a Schmidt trigger circuit operated from a variable phase shifting network supplied from the sixty cycle line. This circuit is followed by two binary counters so arranged that a pulse whose rate is 60, 30, or 15 cps can be chosen at will. When the length of the pulse is made 670 microseconds, the duty cycle is therefore 25 to 1, 50 to 1, or 100 to 1.

On the integrator chassis this pulse is used as one input to an anticoincidence circuit. The integrator supplies the other input to this circuit. The purpose of this is to block the pulse whenever the

integrating capacitor is being discharged. It was found necessary to do this because the soakage in the dielectric of the integrating capacitor amounted to several percent unless the capacitor was discharged for a period of one-half second or longer. After passing through the anticoincidence circuit, the pulse is available to perform the following functions. First, to turn on the scalars. The coincidence circuits used for this purpose are an integral part of the scalars, type 10T1, used by this laboratory. Second, to start the sweep on the monitor oscilloscope. The signal for the vertical plates of the oscilloscope is the voltage developed across a resistor in series with the target current meter. Thus, knowing the voltage sensitivity of the oscilloscope, a continuous monitor of the current pulse supplied to the target is visually available. Finally the pulse is used to supply a signal for the control of the ion source. This is done by using the differentiated and amplified pulse to drive a type R1130B flash tube. The light flash created by this tube is guided by a light shielded lucite tube to the ion source control circuit. Here it is again converted into an electrical pulse by means of a type 931A photomultiplier tube. This pulse starts a one shot multivibrator. The pulse generated by this multivibrator is 600 microseconds long and because of delays in the light flashing circuits it begins a microsecond after the scalars are turned on. This will insure that no protons are supplied to the target before the scalars are ready. Furthermore, the pulse controlling the scalars is variable in length, and so they can be left on somewhat longer than the ion source is in operation. The 600 microsecond pulse is amplified and used to control the bias on two type 811A triode vacuum tubes. These tubes are supplied with a plate voltage of 1500 volts by a power supply

that has an output capacitor of ten microfarads. The ion source is connected in series with these tubes and the power supply. Because of the characteristics of the 811A, a constant current pulse of one ampere is supplied to the arc. Furthermore a high striking voltage is available if needed.

The integrator was calibrated as follows. A constant current source was constructed for which the circuit is shown in Figure 11. The current was determined by measuring the voltage developed across a known resistor with a type K potentiometer, and it was found to vary linearly over a range of 0.1 percent as the integrating capacitor voltage varied from 0 to 100 volts. Thus the average current is suitable for calculations to a high order of precision. The calibration consisted in measuring the time required to charge the integrating capacitor to a voltage predetermined by the integrator. This voltage determined by the integrator was found by using a precision voltage divider and the type K potentiometer. It was found to drift by less than 0.1 percent over long periods of time. In everyday use the power supply voltage of the integrator was measured less accurately through the use of an auxiliary precision meter. All resistances involved were of either the wire-wound or Noboloy type. They were measured several times using a Wheatstone bridge. By repeated measurements the effective capacity of the ten microfarad capacitor used in the carbon determination was found to be 9.60 ± 0.04 microfarads. This is for cycling operation at average charging currents between 5 and 25 microamperes. The effective capacity for single runs where the capacitor remains shorted for a minute or longer is higher, being 9.70 microfarads. The currents used throughout this experiment were high enough to make leakage negligible.

4. Wave Forms of the Current Pulses.

An interesting effect was observed early in the work. This was a difference in the wave forms of the current pulses corresponding to the different mass components of the beam. If the current wave form supplied to the arc is observed, the pulse is typified by that shown in Figure 12a. The decreasing amplitude of the pulse with time is due to the discharge of the output condenser of the arc power supply. If one now observes the pulse appearing on the screen of the monitor oscilloscope when the mass one or proton beam is focused on the target a very similar wave form is obtained. This is shown in Figure 12b, and is of course what would be expected. But if now the mass two or singly ionized molecular beam is observed the pattern is different. This is pictured in Figure 12c. The current form of the mass three component is also shown. Since many fine details of the curves may be due to the nature of the focusing, condition of the arc chamber, and nature of the analyzing magnetic field, only the gross effect of a slow rise for the mass two rather than a rapid one, as in the case of the mass one, was felt to be of any significance. The explanation of this phenomenon was not at first apparent to the author but the work of others coupled with his own leads to the following proposal.

Consider the following experiment. Measure the output currents corresponding to the various mass components as a function of the pressure of the gas in the discharge. The discharge pressure was measured by noting that the system pressure will be proportional to the discharge chamber pressure. Curves taken in this manner are plotted in Figure 13. The general nature of these curves is found to be independent of the

type of ion source [1]. In the case of the P. I. G. source the arc would not operate stably at pressures where the mass one should begin to fall off, but the behavior of the mass two and three components followed the usual trend.

Next consider the following calculation. If the arc current is one ampere and the arc is like those ordinarily studied then there must be about an ampere of positive ions striking the metal surfaces [6]. For the moment let us suppose that an ion stays in the surface of the metal after striking it. Then the following calculation can be made as an order of magnitude for the time required to completely "pump" out of the arc chamber the gas initially in it.

$$\text{Number of molecules available} = 3 \times 10^{19} \frac{\text{mol.}}{\text{c.c.}} \text{ N.T.P.} \times \frac{20 \times 10^{-3} \text{ mm} \times 30 \text{ c.c}}{760 \text{ mm}}$$

$$= 3 \times 10^{16} \text{ mol.}$$

$$\text{Time to remove at one ampere} = \frac{3 \times 10^{16}}{6 \times 10^{12} \times 10^{6}} = 5 \text{ milliseconds}$$

When it is considered that the gas is being supplied to the arc chamber continuously, and that a fraction of the ions probably escape from the metal surfaces after being neutralized, it would not be surprising to have a reduction in the pressure in the arc chamber during the first few hundred microseconds of the pulse followed by a gradual return to normal pressure as equilibrium is established. Referring to the curves of the behavior of the mass fractions as a function of the gas pressure such an effect would indeed lead to wave forms like those observed. Furthermore this pumping action will help explain the difficulty in observing a peak in the mass one component, for an arc chamber starting out at a rather

low pressure might be pumped into a region of pressure too low to support a stable arc. It is regretted by the author that time did not permit checking this argument with more thorough experiments. It is quite possible that studies of ion sources by a pulsed technique such as this could shed considerable light on the mechanics of the discharge.

5. Measurement of the High Voltage.

The high voltage used to accelerate the ions was measured by the current in a resistor column. The column consisted of a 20 megohm resistor and a 100 megohm resistor in series. The precision 20 megohm resistor was calibrated by Mr. Cartwright of our calibration laboratory, and was in turn used to calibrate, by a comparison method, the oil enclosed column of precision wire-wound resistors of 100 megohms total resistance. The current in the column was measured by a Weston 500 microampere meter of high precision. Whereas this meter reads correctly the average voltage, a correction is necessary because of the pulsed nature of the equipment in order to find the potential available to accelerate the ions.

The high voltage unit may be represented as a battery in series with a resistance representing the total series resistance presented to the current flowing in the beam during the pulse. The meter reads the battery voltage while the resistance is almost entirely in the 500,000 ohm limiting resistor in series with the high voltage unit. The true voltage accelerating the ions will be given by,

$$V_{true} = V_{meter} - 500 \times I$$

provided the duty cycle and correction term are small. Now the total

additional drain, I, is given by the proton current added to the beam current. These currents can be determined to better than ten percent. As the 500,000 ohm resistor is known to ten percent, the correction term is known to within fourteen percent. The correction term amounts to two kilovolts in typical cases, and its error combined with the meter uncertainty of 200 to 300 volts and the variation of the target potential due to the integrator, introduces a probable error of 350 volts in the direct voltage determination.

Besides this direct uncertainty in the voltage, there is an additional source of error arising from the ripple present on the high voltage units. With the currents ordinarily used this ripple appears in the following ways. First, assuming about one and one-half milliampere average drain from the supply, the ripple on the Wappler units operating from the house sixty cycle line is 300 volts. Since the ion source is phased with these units from the same line, and because no attempt was made to determine the relative phasing, one should consider this as a source of random error of 150 volts. Now the booster unit and the focus unit operate from the motor driven generator whose frequency is never quite the same as the line frequency. Thus their ripple which comes to about 450 volts constitutes a spread in the beam energy, but not an error. Thus the probable error in the beam energy is taken to be one-half kilovolt and the beam spread to be at least one-half kilovolt. The high voltage stability is also about one-half kilovolt, and hence in the determination made with this accelerator the error in the beam energy will be given as 750 volts.

PART II

CONSTRUCTION AND CALIBRATION OF THE COUNTER

1. The Scintillation Counter.

Although the scintillation counter is thought of as a recent development, it was actually one of the earliest detectors used in nuclear physics. For example, every student of physics learns of the work of Rutherford concerning the disintegration of nitrogen when bombarded by alpha particles [9]. In this experiment the reaction products were detected by the scintillations of light they produced on a zinc sulphide screen. These minute flashes were counted visually through a microscope. Because this technique is tedius and inconvenient, the method lost favor in preference to ionization chambers, cloud chambers, and Geiger tubes. In the last few years, however, the idea of viewing the scintillations with a photomultiplier tube developed and was so successful, even with the relatively primitive 931A tubes first used, that rapid development followed. On the one hand the manufacturers of photomultipliers developed new type tubes with large cathode areas and high sensitivity. On the other hand the range of phosphors was expanded to include crystals transparent to their own radiation, liquids with dissolved phosphors, and powders of various properties.

2. Development of the Counter Used in this Experiment.

Attempts to construct a counter suitable for this experiment were first centered about the use of a liquid phosphor. A glass chamber was constructed with a small re-entrant hole for the proton beam to enter. The target was placed at the bottom of this hole and was thus completely surrounded by the phosphor. The chamber was filled with a saturated

solution of terphenyl in xylene. This solution is reputed to be one of the best of the liquid phosphors [10]. The counter was checked with thorium, radium, and cobalt sources and seemed to operate satisfactorily. A determination of the C^{13} cross section at 130 kilovolts gave inconclusive results. In order to get an estimate of the counter efficiency, the yield from boron was determined and the results were compared with those obtained by Tangen [11]. Although he gives no absolute cross sections, estimates based on his probable counter efficiency, when compared to the yield obtained in our experiment showed the counter to have an efficiency of four percent. Using the absorption coefficient for fourteen million volt radiation in xylene, 0.012 cm^{-1}, and the available absorption length of three centimeters, a three and one-half percent efficiency would have been calculated. In view of the result finally obtained for carbon, the counting rate should have been about twice background in the C^{13} determination. A careful re-analysis of the data shows that the initial counting rate was not far from this value but that it fell off as the experiment progressed. The failure is now traced to two causes. First the vacuum system was not operating properly and the trapping was insufficient. This was the only target used which showed signs of being coated after use, and this coat will explain the gradual falling off of the counting rate. Second, the background was high, because no lead shielding was used in this initial work. Later results have shown a forty percent reduction might have been obtained by the use of two inches of lead shielding. Also the absorption of terphenyl solution is low for the eight million volt radiation of C^{13}. This means the use of a relatively large volume in order to

get a reasonable efficiency. However, a large volume also means that a large cross section will be presented for the absorption of cosmic radiation and other background sources. Because of this latter reason, the terphenyl-xylene phosphor was abandoned and attention was turned to crystals of sodium iodide activated with thallium.

Sodium iodide was selected because it has the following desirable properties: (a) It has a large light output for a given amount of energy lost in the crystal. (b) It has a high density which means that a high absorption can be obtained in a small volume of material. (c) It has a constituent, iodine, of high atomic number which gives a good probability for the formation of pairs. (d) It is readily available compared to crystal phosphors as a whole. The chief disadvantages of the crystal are: (a) It is very hygroscopic and must be kept immersed in oil. (b) The decay time of the scintillations is about one-half microsecond which is long compared to most phosphors. In Figure 14 are plotted the calculated total absorption cross sections for xylene and sodium iodide as a function of incident gamma ray energy.

The first sodium iodide counter tried used a crystal of dimensions one-half inch thick by one inch square. This gave much lower background counting rates than the terphenyl solution. The counter was then tried on carbon and gave positive results.

Immediately the idea of increasing the solid angle by placing smaller crystals about the target in addition to the single large crystal was suggested. It was done and appreciably higher efficiencies were obtained. Doing so, however, accentuated a difficulty already observed with the first crystal counter. When the range, in the crystal, of the electrons created by the gamma radiation is about the same as the

dimensions of the crystal, edge effects become important. The chief result is a preponderance of small pulses. This is undesirable for it makes the extrapolation of an integral bias curve to zero bias difficult and also requires a lower bias setting for the same counting rate. A low bias setting always results in more background. The following formula for computing the range of electrons in sodium iodide is correct for energies between one and ten million volts.

Range in mm = 1.5 times energy in Mev.

Thus for seven million volt electrons the range is one centimeter. For this reason a third counter was constructed in which the crystal was a one inch cube. It is also necessary to select the photomultiplier tube as the cathode surface varies a great deal from tube to tube. Many tubes are sufficiently poor to destroy the advantage gained by going to larger crystals.

3. Description of the Construction and Calibration of the Final Counter.

Figure 15 shows a drawing of the counter arrangement used. The sodium iodide crystal was held in place by lucite spacers, not shown, and the interior of the lucite cup was filled with sodium dried mineral oil. The crystal was cleaned with a solution of acetone and xylene before assembly. In order to insure good optical contact between the lucite cup and the cathode of the photomultiplier tube, a thin layer of light celvacene grease was formed between them. In actual operation the assembly was rendered light tight by wrapping black tape about the lucite viewing window. It was found necessary to shield the photomultiplier magnetically from stray fields. The shields shown, consisting of one layer of mu metal

and several layers of two mil transformer iron, proved sufficient.

The photomultiplier was operated at a supply voltage of 900 volts. This was distributed equally among all the dynodes except the first. By operating the first dynode at a higher voltage better pulse height distribution was obtained. The pulse was taken from the last dynode into a cathode follower mounted on the photomultiplier support. The output of the cathode follower was carried to an amplifier type 10T2. The output of this amplifier was sent to pulse height discriminators and scalars.

Photomultiplier tubes are very sensitive to many parameters and it is not unusual for their gain to vary considerably from day to day. For this reason, and also to provide a calibration of the energy scale, the following scheme was developed. A source was constructed from Co^{60}. In the lucite insulator mounted against the end plate of the phototube shield a hole was drilled to fit this source, and thus it was possible to irradiate the crystal with an unknown but fixed amount of radiation. The integral bias curve for the Co^{60} source was a straight line over a considerable part of its range. This is shown in Figure 16. The usefulness of this fact lay in the possibility of checking the counter efficiency and amplifier gain by determining the straight line portion with two or three points and then checking the intercepts on both axes. The y axis intercept checks the efficiency, and was found to be 45,500 counts per minute over a wide range of phototube voltages and amplifier gains. The x intercept checks the amplifier and phototube gain. The gain was always adjusted to make the intercept 97.5 volts.

With the amplifier gain adjusted in this manner, the step attenuator was next changed to reduce the gain by a factor of eight. The x intercept of the Co^{60} then became 12.5 volts. With the amplifier so adjusted, integral

bias curves were taken for a number of different gamma ray energies. These curves are shown in Figure 17. The straight line portion of each of these curves was extrapolated until it intersected the x axis. These intercepts were then plotted as a function of gamma ray energy and the result is also shown in Figure 17. Considering the empirical nature of this procedure the deviations from a straight line in the resulting curve are remarkably small. As accurate determinations of gamma ray energies are not essential in this experiment, the curve was considered to be a satisfactory relation.

Assuming the bias curves should be straight lines, it is possible to give qualitative interpretations for their deviations from straight lines. In the case of low energy gamma radiation the curves deviate at both ends. The high energy deviation is probably due to the photo absorption of the radiation. This absorption amounts to about twenty percent of the total absorption at two million volts. The sharp break at a bias corresponding to an electron energy of two hundred and fifty kilovolts is attributed to the back scattered Compton radiation from the surroundings of the crystal. It is not unreasonable to expect this curve to approximate a straight line for the absorption is mostly by Compton effect, which at this energy should give very closely the integral bias curve found. On the other hand the bias curves for the higher energy gamma radiation are not so easily explained, and it is fortuitous that the extrapolated endpoints are useful parameters for determining the energy. At these energies the ideal bias curve would show a rapid rise followed by a nearly flat plateau. This is because Compton electrons from high energy radiation are nearly monoenergetic. The pair energy is of course monoenergetic. The deviation from this ideal curve is undoubtedly due to edge effects in the crystal. It will be noted that as the energy increases the sharp drop near the endpoint decreases.

This effect has been observed by others [12][13]. The rise of the C^{13} bias curve below a bias of 30 volts is due to a low energy component in the gamma radiation. A much more satisfactory manner of determining gamma ray energies with a scintillation spectrometer is through the use of a differential technique, but as the counting rate expected in the C^{13} reaction at low energies is small this method was not applicable, and the integral method was developed.

The above work was performed using the 3.0 Mev Van de Graaff generator. At the same time an absolute calibration of the counter was attempted using the $F^{19}(p,\alpha\gamma)$ radiation. The gamma radiation from this reaction is 80 percent 6.14 Mev and 20 percent 7.1 Mev at a bombarding energy of 750 kilovolts. If one takes into account the slight angular distribution of two of the levels involved, the forward yield for the reaction at 750 kilovolts is 10^{-7} gamma rays per proton for a thick CaF_2 target. At one million volts the yield is 7.13×10^{-7} and the radiation is slightly harder [14]. Before this figure can be directly applied to the data taken a correction is needed. Because of the need in the carbon determination to obtain as large a solid angle as possible, there was only one and one-quarter millimeters of aluminum between the target surface and the crystal. Besides the gamma radiation there are a considerable number of nuclear pairs from the reaction. Their energy is 5 Mev. The amount of aluminum between the target and crystal is only sufficient to reduce this energy by 600 kilovolts. Therefore a portion of the pairs are certainly counted. The yield of pairs obtained at various bombarding energies has been given by Streib, Fowler, and Lauritsen [15]. They give the integrated yield of particles from pairs up to 800 kilovolts as 0.013×10^{-7} for a thick CaF_2 target. Referring to the excitation curve given in their paper, one may

estimate the yield at 750 kilovolts as one half this, or 0.007×10^{-7}. The yield of particles at one million volts is 0.10×10^{-7}. If the counter subtended the same effective solid angle for the pairs as it does for the gamma radiation, then one could estimate from the absorption coefficient of the sodium iodide, and the distance available for absorption, that the gamma radiation equivalent of the pairs would not be greater than three times their actual yield. Because of the greater absorption in the aluminum at oblique angles for the pairs their effective solid angle must be less. It has arbitrarily been taken as two-thirds that for the gamma rays. With this correction the effective yields at the two bombarding voltages are 1.02×10^{-7} and 7.43×10^{-7} respectively. The yields observed were:

750 kev	49,000 counts for 1.05 microcoulombs
1000 kev	422,000 counts for 1.05 microcoulombs

Now these are in the ratio of 8.6 to 1, whereas the reported yields are in the ratio of 7.34 to 1. In order to make sure that the pair correction was not larger than calculated, another experiment was performed in which absorber was placed between the counter and target to absorb all pairs. While this cannot give an absolute calibration for the counter, it should give the correct ratio for the gamma ray yields at the two bombarding voltages. The results of this experiment gave a ratio of 8.5 to 1 with absorber out, while with the absorber the ratio was 8.22 to 1. The author is of the opinion that the reported yields for the resonances below 750 kilovolts are too high. His data would give the yield at 750 kilovolts as 8.9×10^{-8} if the one million volt value is taken 7.13×10^{-7}.

In order to proceed with the calculation the following assumptions were made: (a) As reported by Chao, et. al[14] the yield at one million volts is 7.13×10^{-7}. (b) The ratio of yield at one million volts to 750 kilovolts is 8.22 to 1 as determined above. (c) The pair correction

at 750 kilovolts is two percent. This procedure was followed because the pair correction is smaller at 750 kilovolts whereas the yield is better known at one million volts. With these assumptions, and the yield found above, the efficiency of this counter for 6 Mev radiation is 8.45 percent.

As a check on this calibration, thick target excitation and bias curves were made using graphite as the target. At 500 kilovolts the extrapolated yield for the bias curve is 20,400 counts for 55.0 microcoulombs. In drawing the bias curve the points below seven volts have been neglected because the positrons from the disintegrations of the N^{13} would then be counted. These positrons have a maximum energy of 1.25 Mev. Two corrections must be applied in computing the yield of the reaction from this data. First, the counter efficiency is greater for the 2.3 Mev radiation from the C^{12} than for 6 Mev radiation, because of the increase in the adsorption coefficient of the sodium iodide. Second, if the excitation curve obtained from the positron data of J. D. Seagrave is reviewed, it is seen that the bombarding energy of 500 kilovolts is not sufficient to give the full thick target step. Making these corrections gives the yield of the C^{12} reaction at one million volts as 7.05×10^{-10} which is to be compared with the value 7.2×10^{-10} reported in the literature (16).

An assumption made throughout this work is that the efficiency of the counter for different energy gamma radiation is proportional to the absorption coefficient of the phosphor. It is possible that at higher energies the scattered particles from the surroundings might contribute considerably to the yield. It is sufficient to point out the satisfactory result obtained in an extrapolation from 6 Mev to 2 Mev, and then to claim that no greater error can result in the extrapolation from 6 Mev to 8 Mev.

PART III

CAPTURE CROSS SECTION OF C^{13} AT 128 KILOVOLTS

1. Targets.

The C^{13} targets used in this experiment were made from methyl iodide enriched in C^{13}. This material is supplied by Eastman Kodak. The carbon content is enriched to contain 61 percent C^{13}. The targets themselves were made by a cracking process that resulted in a thin hard film of carbon on a polished tantalum strip. The proton thickness for 128 kilovolt protons was greater than that needed for a thick target. This process was developed by J. D. Seagrave and is adequately described in his thesis. Through his kindness, targets were made available for this experiment. These were prepared for use by punching a disc from the tantalum strip. This disc would then fit snuggly against the end of the target chamber. The targets held up well but after long bombardment they would occasionally flake off. They were inspected after each set of runs.

The enrichment factor of the targets was checked by comparing the yield of a thick graphite target at the 1.7 Mev resonance of C^{13} with the yield from one of the enriched targets. This data gave an enrichment factor of 51. The actual content is 60 percent when 1.1 percent is taken as the normal abundance, and the 20 kilovolt enriched target is corrected to a thick target. The probable error in this determination is 3 percent and is due to uncertainties in the values of the integrator capacitors and counter voltage fluctuations. In a similar experiment J. D. Seagrave found the content to be 64 percent with a probable error of 5 percent. These determinations are considered to be in satisfactory agreement, and the value of 61 percent given by Eastman will be used.

2. Reduction of the Data.

After shielding the counter with two inches of lead a good fraction of the background was due to pulses larger than any that could result from C^{13}. These are presumably due to cosmic radiation. This information can be used to greatly reduce the uncertainty in the background correction. In addition the proton current is off most of the time because the beam is pulsed. This time can be utilized for measuring the background. This is fortunate, for any locally arising background is then much more likely to be properly corrected for. To take advantage of these possibilities four discriminators and four scalars were used for collecting the data. The first scalar was turned on only with the beam and its discriminator was set to the bias voltage at which a reading was desired. The second scalar was on all the time and its discriminator was set to the same bias as the first. The third scalar was turned on only with the beam and its discriminator was set to a bias too large to count C^{13} pulses. The fourth scalar was turned on all the time and its discriminator was set to the same bias as the third. Designate the counts collected by these scalars as C_1, C_2, C_3 and C_4, respectively. The data C_3 and C_4 may be subtracted from C_1 and C_2 for they represent pulses known to be too large. The differences $(C_1 - C_3)$ and $(C_2 - C_4)$ then form the raw data. Designate them by n_o and N_o respectively. The quantity $(N_o - n_o)$ contains nothing but the true background for a time proportional to $(1 - \tau)$ where τ is the duty cycle. Thus the background while the counter is on, is,

$$\tau \frac{N_o - n_o}{1 - \tau}$$

The counts corresponding to the C^{13} disintegrations are given by,

$$n = n_o - \tau \frac{N_o - n_o}{1 - \tau} = \frac{n_o - \tau N_o}{1 - \tau}$$

The statistical error in $\frac{N_o - n_o}{1 - \tau}$ is $0.7 \sqrt{\frac{N_o - n_o}{1 - \tau}}$

for the quantity under the radical is the actual number of counts expected. The statistical error in the fraction of these counts that will appear as background when the beam is on is therefore,

$$0.7(N_o - n_o) \frac{\tau}{1 - \tau} \sqrt{\left\{ \frac{\left[\frac{\tau}{1 - \tau} (N_o - n_o) \right]^{\frac{1}{2}}}{\frac{\tau}{1 - \tau} (N_o - n_o)} \right\}^2 + \left\{ \frac{\left[\frac{N_o - n_o}{1 - \tau} \right]^{\frac{1}{2}}}{\frac{N_o - n_o}{1 - \tau}} \right\}^2}$$

$$= 0.7 \frac{\tau}{1 - \tau} (N_o - n_o)^{\frac{1}{2}} (1 + \tau)^{\frac{1}{2}}$$

Therefore the statistical error in n is given by,

$$0.7 \left[n_o + \tau (1 - \tau)^{-1} (1 + \tau) (N_o - n_o) \right]^{\frac{1}{2}}$$

If $\tau << 1$ and if $n_o < N_o$, as is true for this experiment then the error is given by the approximate formula,

$$0.7 (n_o + \tau N_o)^{\frac{1}{2}}$$

Therefore the computational equation used in reducing the data is,

$$n = \frac{n_o - \tau N_o}{1 - \tau} \pm 0.7 (n_o + \tau N_o)^{\frac{1}{2}}$$

The yield can be determined by using the counter calibration obtained from fluorine, or it can be determined, assuming the yield as known at 700 kilovolts, by comparing the counter yield at the lower voltage with the counter yield at 700 kilovolts. When the yield has been calculated the cross section can be found by using the method of Hall and Fowler [3]. This yields the equation,

$$\sigma = \frac{3Y\epsilon}{fE^{3/2}}\left[1 + \frac{E^{1/2}}{Z_o}\right]$$

where f represents the fraction of C^{13} in the target, ϵ the stopping power of carbon as given by Bethe, and E the energy of the bombarding protons in Mev. This equation is found by evaluating the following integral assuming ϵ is constant,

$$Y = \int_0^E \frac{\sigma}{\epsilon}\, dE$$

The assumption is fairly good, for ϵ is nearly constant from 90 kilovolts to 130 kilovolts, and σ drops so rapidly that the contribution below 90 kilovolts is of no importance. Hall and Fowler give as an approximate form for σ ,

$$\sigma = \frac{a}{E}\, e^{-\frac{Z}{E^{1/2}}} \times 0.99$$

This is derived from the asymptotic form of the penetration factor [3].

3. The Data.

The following table gives the pertinent data obtained in the experiment.

TABLE I

Bias	C_1	C_2	C_3	C_4	Charge microcoulombs	True counts per 1000 microcoulombs
10	63	5	643	182	26,400	1.84 ± 0.22
15	66	6	484	230	35,200	1.54 ± 0.16
20	65	4	602	303	48,400	1.21 ± 0.13
25	61	5	512	282	46,600	1.09 ± 0.12
30	73	13	745	454	70,400	0.759 ± 0.081
40	44	9	456	326	48,400	0.665 ± 0.089
50	21	3	314	228	38,700	0.417 ± 0.084

Voltage 128 ± 0.75 kilovolts

τ = 0.0227

These data are plotted in Figure 18. Making use of the counter efficiency of 8.45 percent and the target enrichment of 61 percent, the yield of the hard component of the C^{13} radiation at 128 kilovolts is,

$$\frac{1.24 \text{ counts}}{1000 \text{ microcoulombs}} \times \frac{1}{0.61} \times \frac{1}{0.0845} \times \frac{1}{6.24 \times 10^{+12}} \frac{\text{microcoulomb}}{\text{protons}}$$

$$= 3.8 \times 10^{-15} \frac{\text{gammas}}{\text{proton}}$$

Noting that the soft radiation is three to four million volts in energy the yield of the soft radiation may be given as,

$$\frac{1.06}{1000} \times \frac{1}{0.61} \times \frac{1}{0.0845} \times \frac{1}{6.24 \times 10^{+12}} \times \frac{1.21}{1.34} = 2.9 \times 10^{-15} \frac{\text{gammas}}{\text{proton}}$$

The cross sections corresponding to these yields are,

$$\sigma_{\text{hard}} = 3.8 \pm 0.76 \times 10^{-33} \text{ cm}^2$$

$$\sigma_{\text{soft}} = 2.9 \pm 0.58 \times 10^{-33} \text{ cm}^2$$

If the soft radiation is due to a two step cascade the cross section for disintegration is,

$$\sigma_{total} = 5.25 \times 10^{-33} \text{ cm}^2$$

If it is due to a three step cascade,

$$\sigma_{total} = 4.8 \times 10^{-33} \text{ cm}^2$$

Figure 20 shows a bias curve made using an ordinary graphite target at a bombarding energy of 700 kilovolts. The soft radiation is mostly from C^{12}. By comparing the yield of the hard radiation from this target at 700 kilovolts with the yield of hard radiation from the enriched target at 128 kilovolts, the ratio of the yields of the hard radiation at these two energies may be given.

$$\frac{Y_{\text{hard } 700}}{Y_{\text{hard } 128}} = 55.5 \times \frac{2600 \text{ counts}}{55 \text{ microcoulombs}} \times \frac{1000 \text{ microcoulombs}}{1.24 \text{ counts}} = 2.2 \pm 0.26 \times 10^6$$

The errors have been estimated as follows. In the ratio just quoted only the counting rates, the values of the charges, and the enrichment factor enter directly. The values of the charges are known to better than one percent. The statistical and extrapolation error at 700 kilovolts is not more than four percent. The statistical and extrapolation error at 128 kilovolts is ten percent. The enrichment factor is known to within a few percent. Therefore the error given for the ratio is twelve percent.

The cross section is less accurately known, and the various errors are:

(1) The extrapolation and statistical error is ten percent.

(2) The error in the charge is one percent.

(3) The error in the counter calibration is ten percent.

(4) The error in the enrichment factor is two percent.

(5) The stopping cross section for carbon may be in error by as much as ten percent.

The effect of these errors is an uncertainty of twenty percent in the cross section.

A number of checks were made to determine if the gamma radiation observed was indeed due to C^{13}. First, a C^{12} target prepared in exactly the same way as the C^{13} target was used and the yield was found to be background. Second, the possibility of target contamination was eliminated by two sets of experiments. One of these sets consists of the experiments made at higher energies; there was at no time any indication of radiation from other reactions. The other experiment was the determination of the excitation curve at 128 kilovolts. This is shown in Figure 21. The points shown on this curve were obtained early in the work and have rather large statistical errors. Now,

$$Y = \frac{2\sigma E^{3/2}}{\epsilon Z_o} \quad \text{approximately}$$

and,

$$\sigma = \frac{a}{E} e^{-\frac{Z_o}{E^{1/2}}}$$

thus,

$$Y = AE^{1/2} e^{-\frac{Z_o}{E^{1/2}}}$$

By plotting the observed yield with the abcissa proportional to the inverse of the square root of the energy, and the ordinate to the logarithm

of the yield, a straight line will result over a limited region. The best straight line, fitting the data by least squares, has a slope of 52 ± 2 degrees while the theoretical slope for boron is 49 degrees and for carbon is 54 degrees. Nitrogen and oxygen would not give trouble as contaminants because their cross sections are too small, and the possibility of fluorine contamination was eliminated in the work done at higher energies.

It is conceivable that a locally generated electrical interference might be synchronized with the proton pulse. This type of background would not be detected by the ordinary method of making the background correction if it were not fairly large. Therefore the third check consisted of backgrounds taken with a C^{12} target or in having the beam intercepted by the beam chopper. At no time was a statistically signigicant synchronized background observed.

4. Nature of the Radiation at Higher Energy.

It is possible to make some prediction of the cross section to be expected at 128 kilovolts from the nature and yield of the reaction at higher energy. There are many resonances, but only two are of sufficient strength and breadth to contribute to the cross section at 128 kilovolts. These are the well known resonance at 554 kilovolts, and a broad resonance at 1.25 million volts.

It is not known whether these resonances will interfere at the low energy, and so for a comparison with the observed results they will be studied separately. The most useful tool for doing this is the single level Breit-Wigner dispersion formula,

$$\sigma = \pi \lambda\!\!\!^{-2} \frac{\omega \Gamma_\gamma \Gamma_p}{(E - E_R)^2 + \frac{\Gamma^2}{4}}$$

$\lambda\!\!\!^{-}$ is the wavelength of the incident proton in the center of mass system, $\omega \Gamma_\gamma$ is a factor nearly independent of energy, E_R is the energy of the bombarding proton at resonance, E is the actual bombarding energy, Γ is $\Gamma_\gamma + \Gamma_p$, and finally Γ_p is given by $P(E)^{\frac{1}{2}}G$ where $P(E)^{\frac{1}{2}}$ is the penetration factor while G is the width at one million volts without barrier. $P(E)^{\frac{1}{2}}$ has been tabulated by Christy and Latter as a function of target nucleus and bombarding energy [18]. At low energies Γ_p becomes very small and thus Γ may be neglected in comparison to $(E - E_R)$. For purposes of extrapolation the equation may be re-expressed as,

$$\sigma = \frac{E_R}{E} \times \frac{P(E)^{\frac{1}{2}}}{\left[P(E)^{\frac{1}{2}}\right]_R} \times \left[\frac{\Gamma_{pR}}{E - E_R}\right]^2 \times \frac{\sigma_R}{4}$$

where $\pi \lambda\!\!\!^{-2}$ has been given by,

$$\pi \lambda\!\!\!^{-2} \left[\frac{A_1 + 1}{A_o}\right] (2\mu E)^{-1}$$

and μ is the reduced mass of the system.

The integral bias curves at 554 kilovolts and also at 1.25 million volts taken with a thin target are given in Figure 19. Except for the very low energy tail on the higher energy curve, they are of the same nature as the curve at 128 kilovolts. They both show about thirty-five percent total soft radiation as compared to forty-three percent for

128 kilovolts, but the error on the latter figure is sufficient to rule out attaching any importance to the difference. J. D. Seagrave has found the widths of the resonances as 32.5 kilovolts for the lower resonance and 500 kilovolts for the higher resonance. The best values available for σ_R are $\sigma_{554} = 1.44 \times 10^{-27}$ cm^2 and $\sigma_{1.25} = 0.062 \times 10^{-27}$ cm^2. These are calculated from total yields using Geiger tubes [17]. Making use of the extrapolation formula these yield,

$$\sigma = 2.26 \times 10^{-33} \text{ cm}^2$$

and

$$\sigma = 0.89 \times 10^{-33} \text{ cm}^2$$

respectively, at 128 kilovolts. This assumes both resonances are due to s-wave protons. These may be combined to give,

$$\sigma = 3.15 \times 10^{-33} \text{ cm}^2$$

assuming no interference. It is seen that this value as well the bias curves would emphasize the cascade as predominantly a triple, but the evidence is not strong. Furthermore, the measured cross section being greater than that given by the simple extrapolation is in accord with a proposal of R. G. Thomas [19].

REFERENCES

1. R. N. Hall, PhD Thesis, California Institute of Technology (1947).
2. A. Schardt, PhD Thesis, California Institute of Technology (1951).
3. R. N. Hall and W. A. Fowler, Phys. Rev. 77, 197 (1950).
4. R. N. Hall, R. S. I. 19, 905 (1948).
5. J. D. Gow, Radiation Laboratory, University of California (unpublished data).
6. J. Bachus, "The Characteristics of Electrical Disharges in Magnetic Fields", A. Guthrie and R. Wakerling, McGraw-Hill (1949).
7. B. Lax, W. P. Allis, and S. C. Brown, J. Appl. Phys. 21, 1297 (1950).
8. W. C. Elmore and M. Sands, "Electronics", McGraw-Hill (1949).
9. H. Semat, "Atomic Physics", Rinehart & Company (1946).
10. G. T. Reynolds, F. B. Harrison, and G. Salvani, Phys. Rev. 78, 488 (A) (1950).
11. R. Tangen, Kgl. Nord. Vid Selsk, 1 (1946).
12. R. B. Day and R. L. Walker, Bull A. P. S. 26, 12 (1951).
13. W. M. Good, C. D. Moak, G. P. Robinson, and H. Reese, Bull A. P. S. 26, (1950).
14. C. Y. Chao, A. V. Tollestrup, W. A. Fowler, and C. C. Lauritsen, Phys. Rev. 79, 108 (1950).
15. J. F. Streib, W. A. Fowler, and C. C. Lauritsen, Phys. Rev. 59, 253 (1941).
16. W. A. Fowler, C. C. Lauritsen, and T. Lauritsen, Rev. Mod. Phys. 20, 266 (1948).
17. J. D. Seagrave, PhD Thesis, California Institute of Technology (1951).
18. R. F. Christy and R. Latter, Rev. Mod. Phys. 20, 185 (1948).
19. R. G. Thomas, Phys. Rev. 81, 148 (L) (1951).

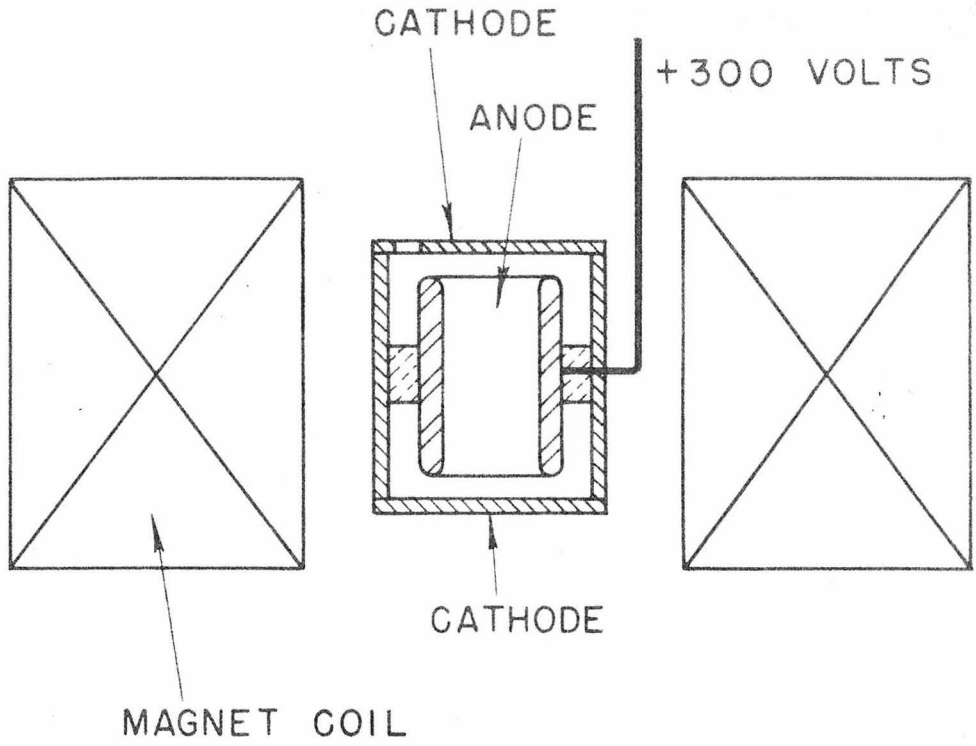

FIG. 1 BASIC ION SOURCE CONSTRUCTION

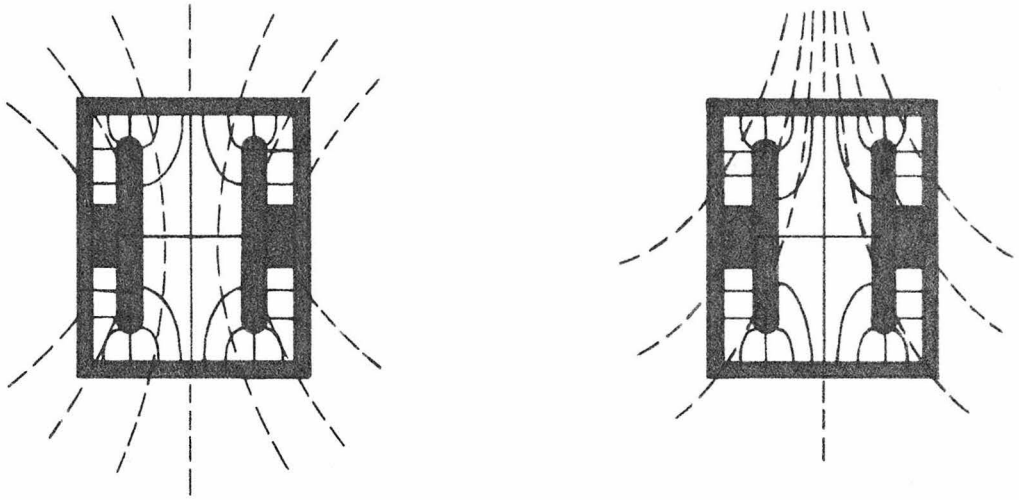

FIG. 2 FIELD CONFIGURATIONS IN ION SOURCE

---- MAGNETIC FIELD

—— ELECTRIC FIELD

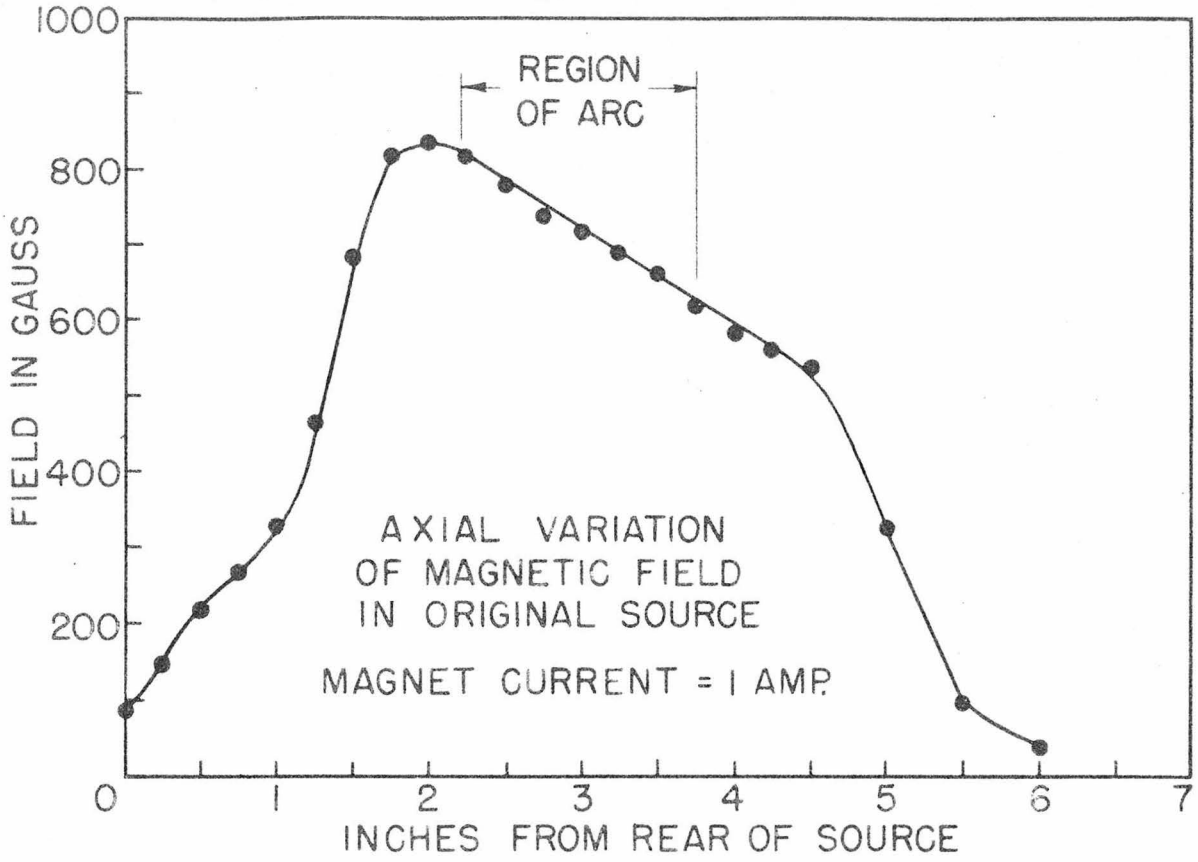
1000
800
600
400
200
0
1
2
3
4
5
6
7
FIELD IN GAUSS
REGION
OF ARC
AXIAL VARIATION
OF MAGNETIC FIELD
IN ORIGINAL SOURCE
MAGNET CURRENT = 1 AMP.
INCHES FROM REAR OF SOURCE

FIG. 3a

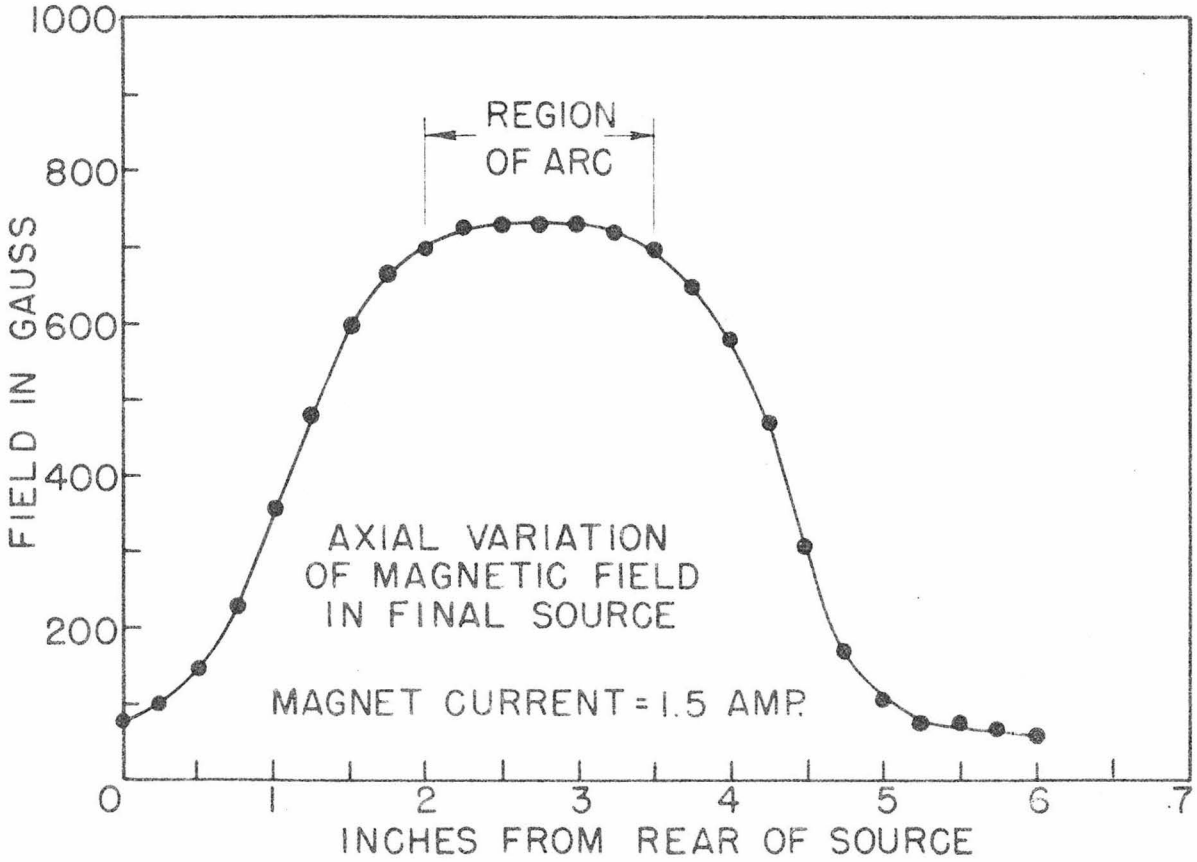
1000
800
600
400
200
0
1
2
3
4
5
6
7
FIELD IN GAUSS
REGION
OF ARC
AXIAL VARIATION
OF MAGNETIC FIELD
IN FINAL SOURCE
MAGNET CURRENT = 1.5 AMP.
INCHES FROM REAR OF SOURCE

FIG. 3b

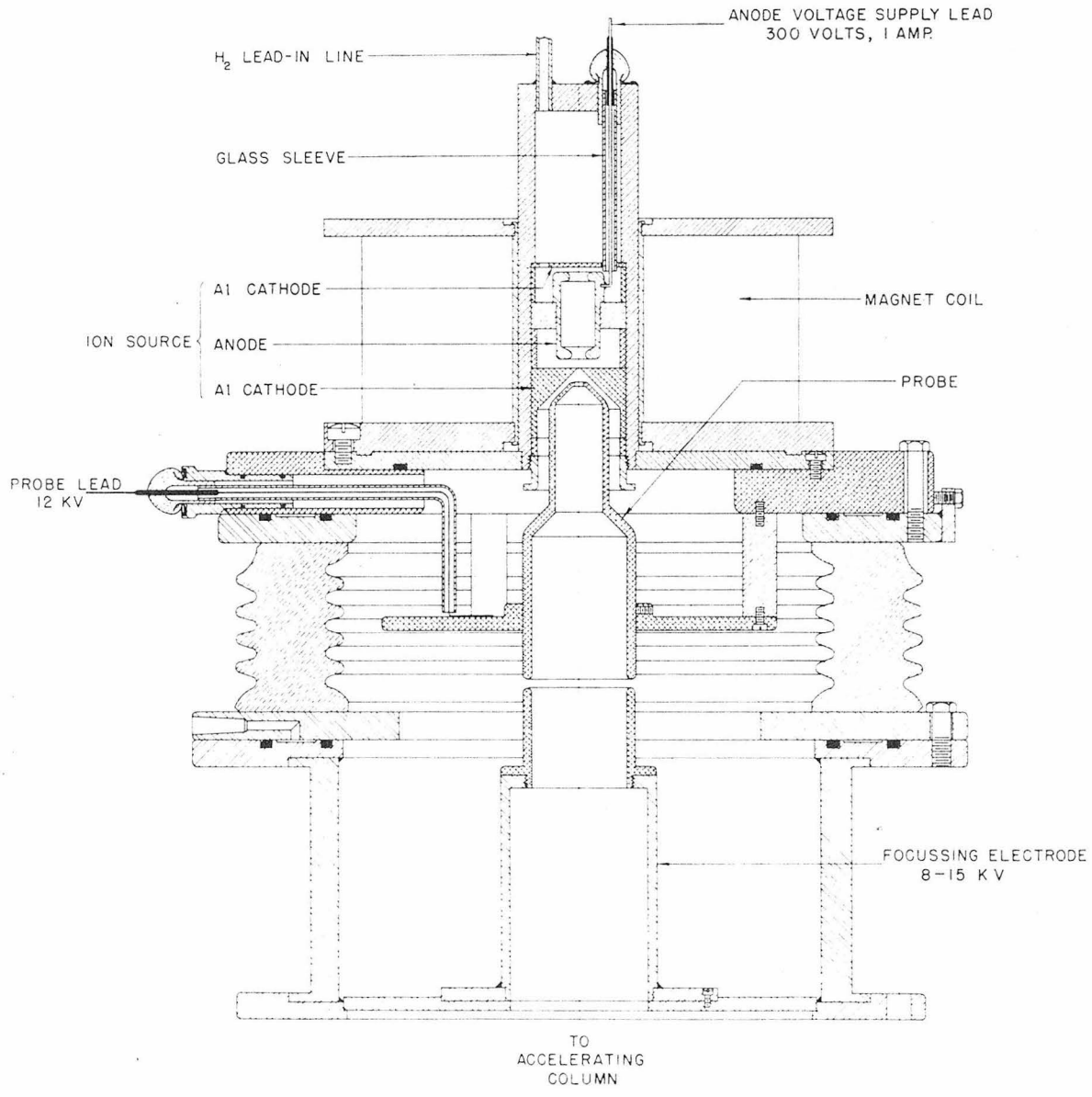

FIG. 4 ION SOURCE ASSEMBLY

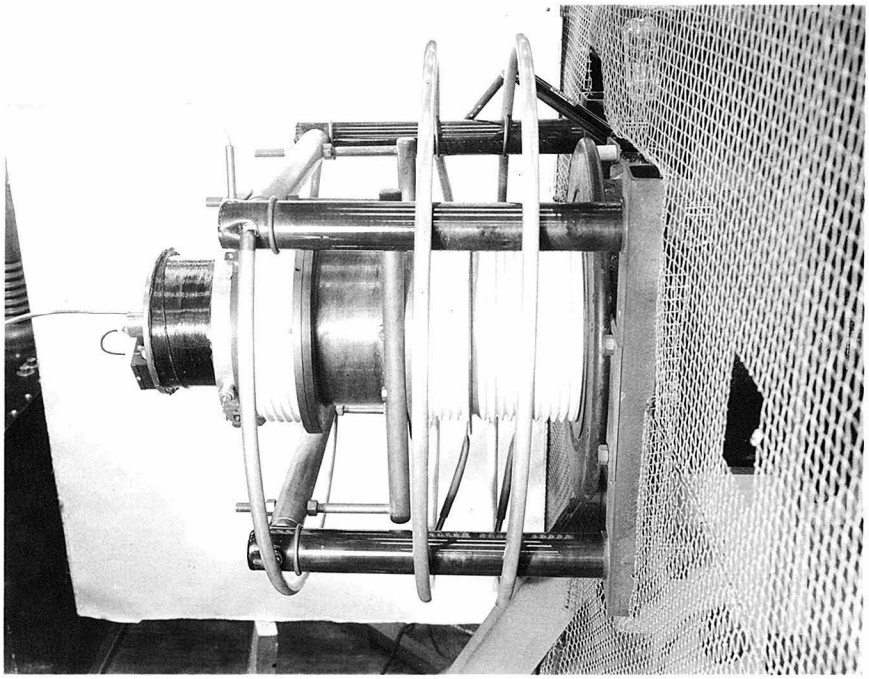

FIG. 5 ACCELERATING COLUMN AND ION SOURCE

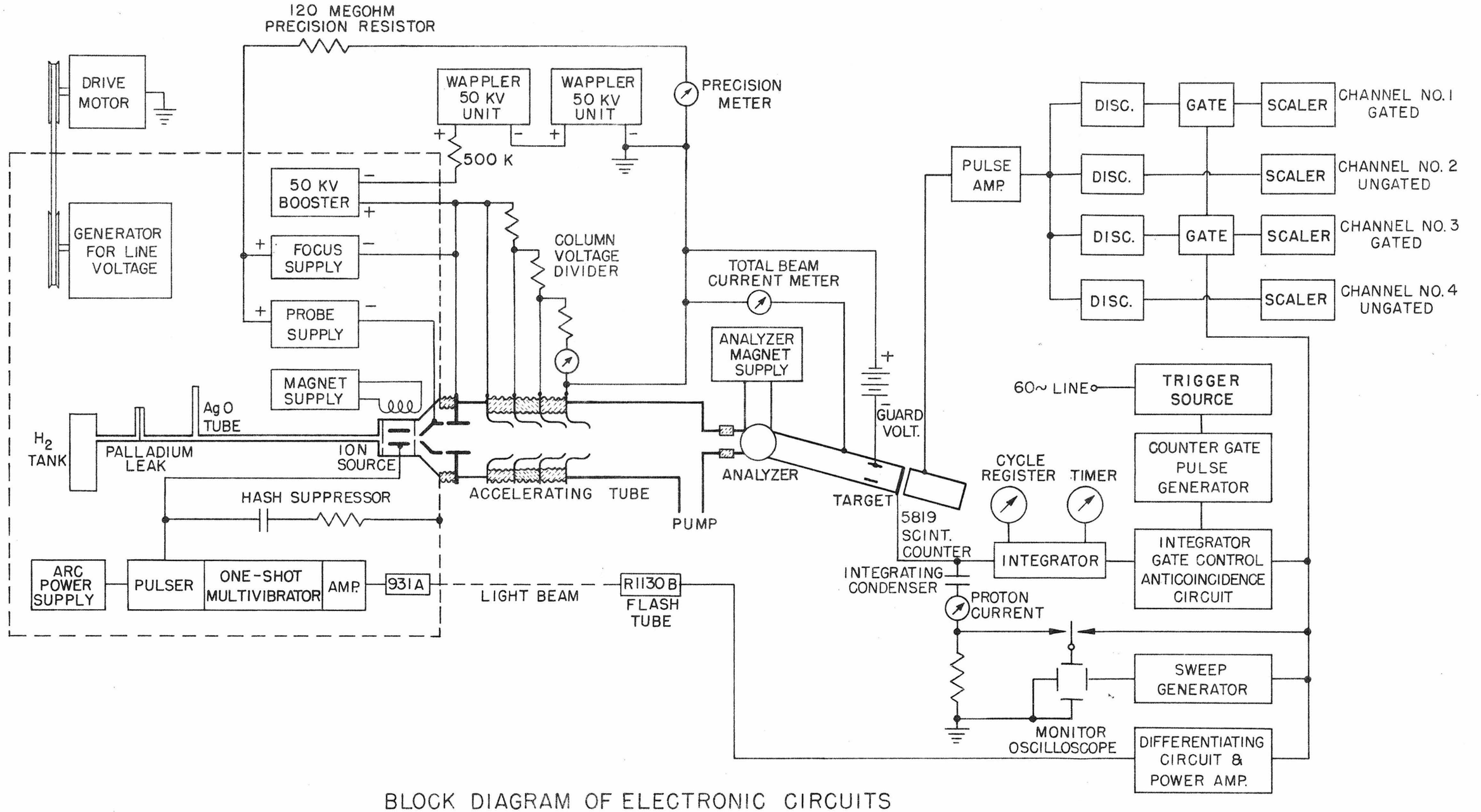

BLOCK DIAGRAM OF ELECTRONIC CIRCUITS

FIG. 6

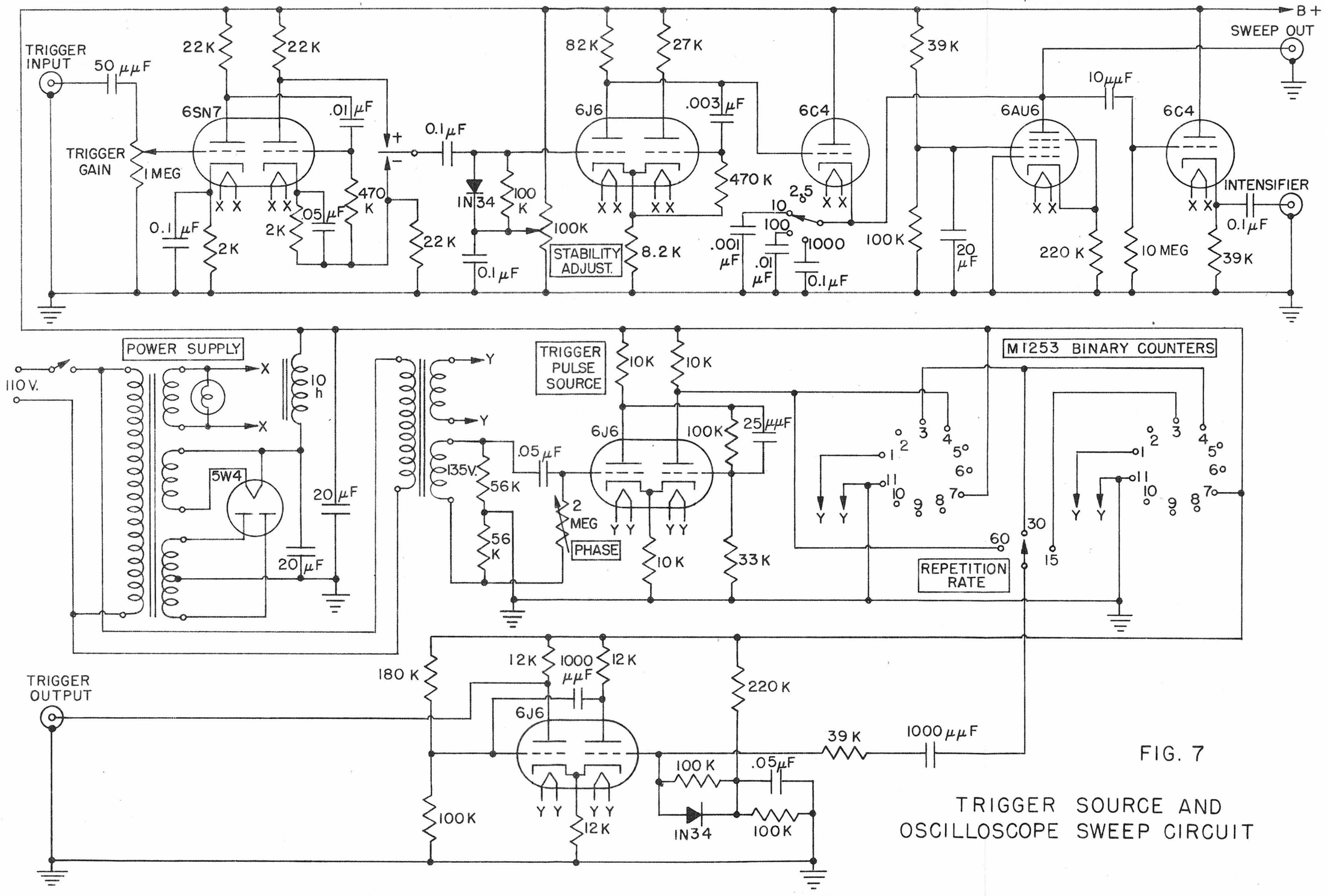

FIG. 7

TRIGGER SOURCE AND OSCILLOSCOPE SWEEP CIRCUIT

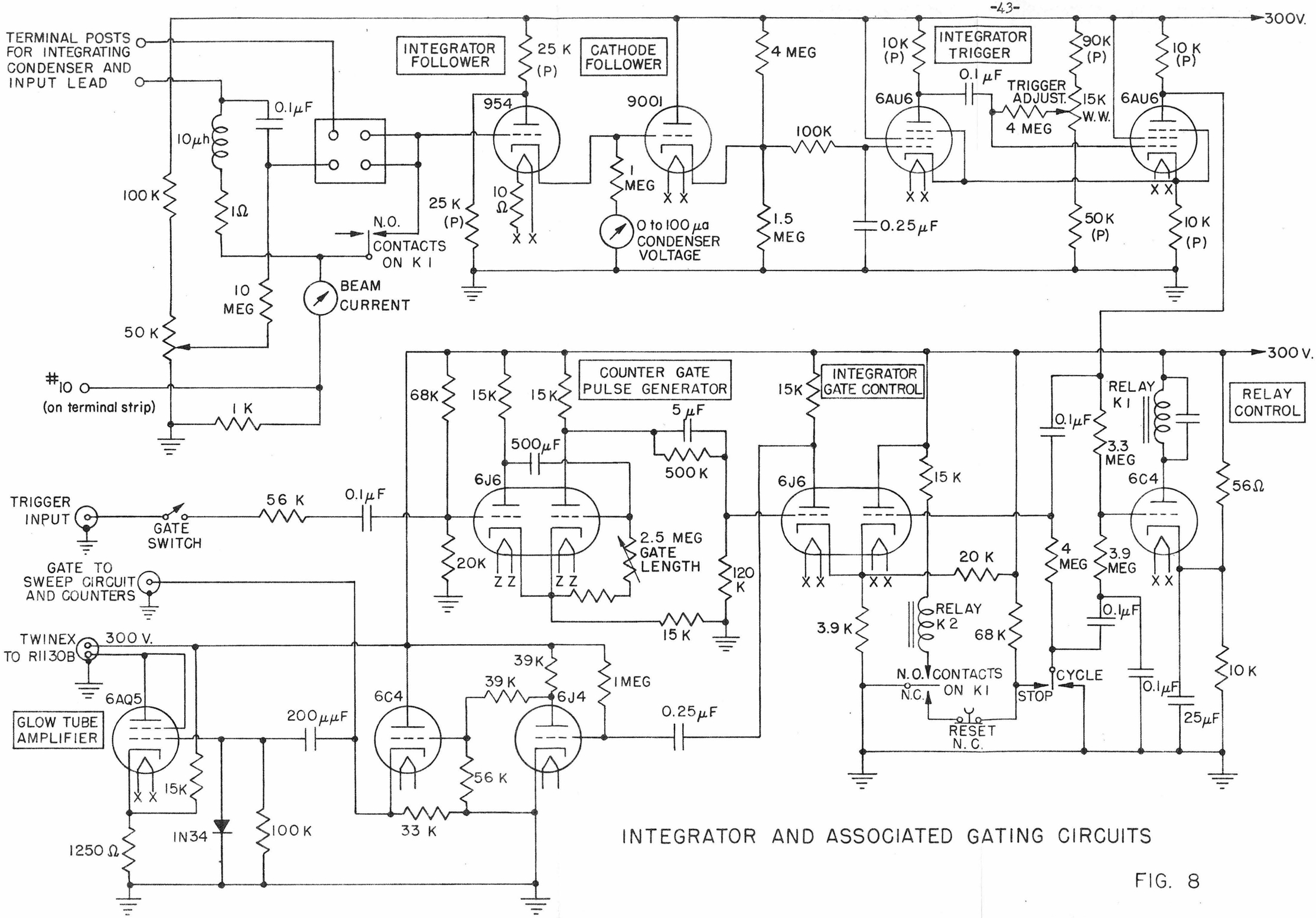

INTEGRATOR AND ASSOCIATED GATING CIRCUITS

FIG. 8

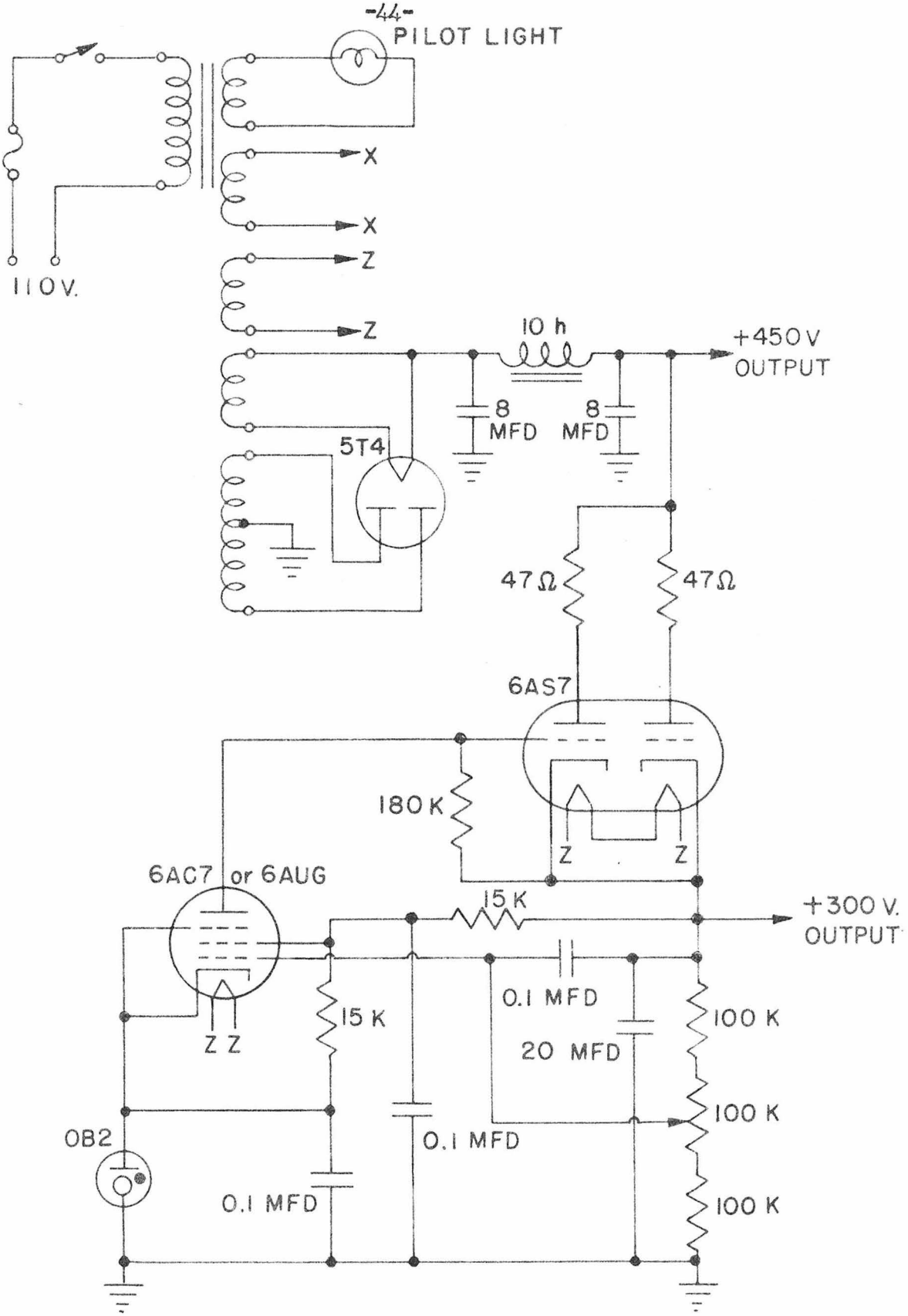

FIG. 9

REGULATED POWER SUPPLY

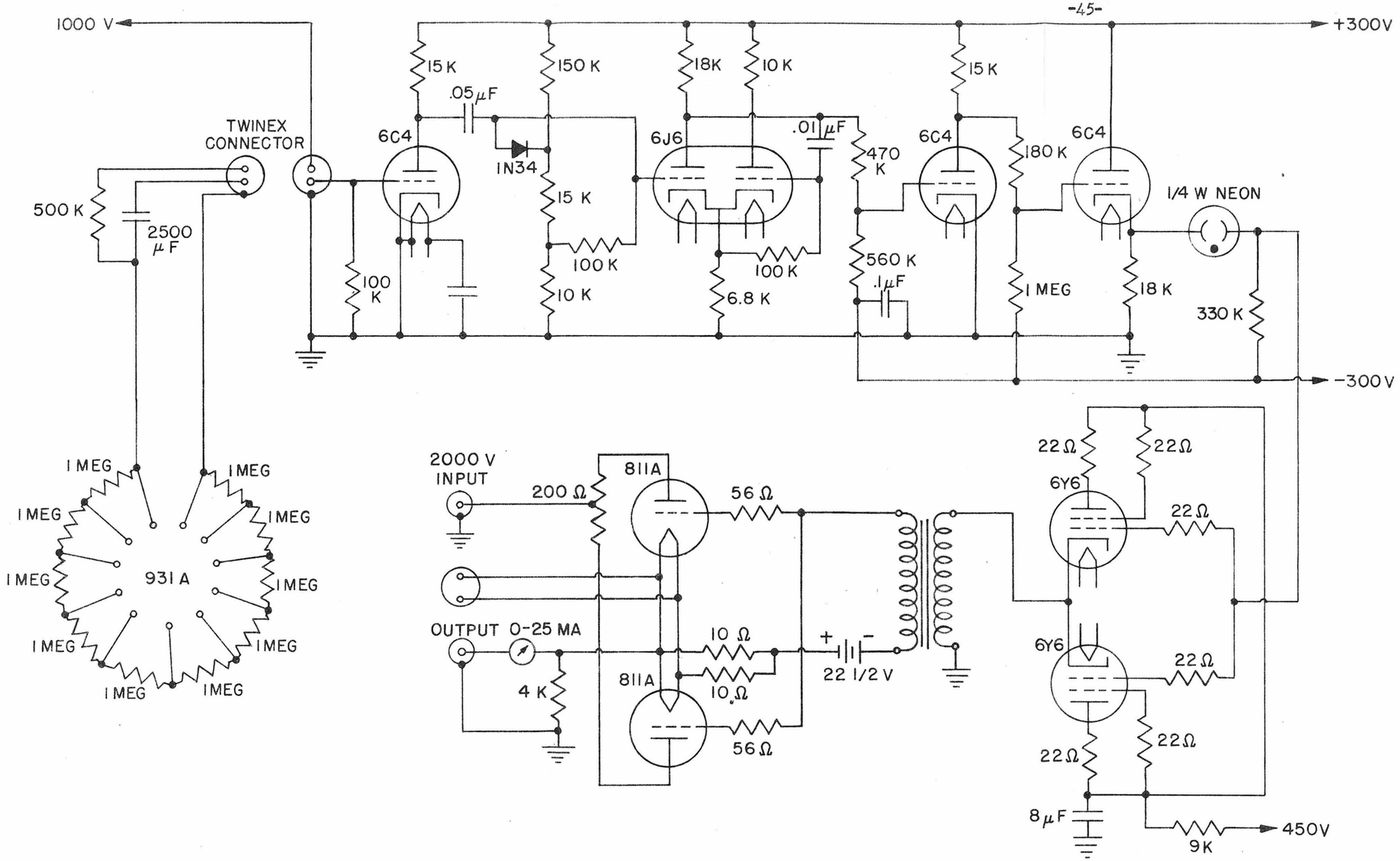

ION SOURCE PULSE LENGTH MULTIVIBRATOR
AND POWER PULSE AMPLIFIER

FIG. 10

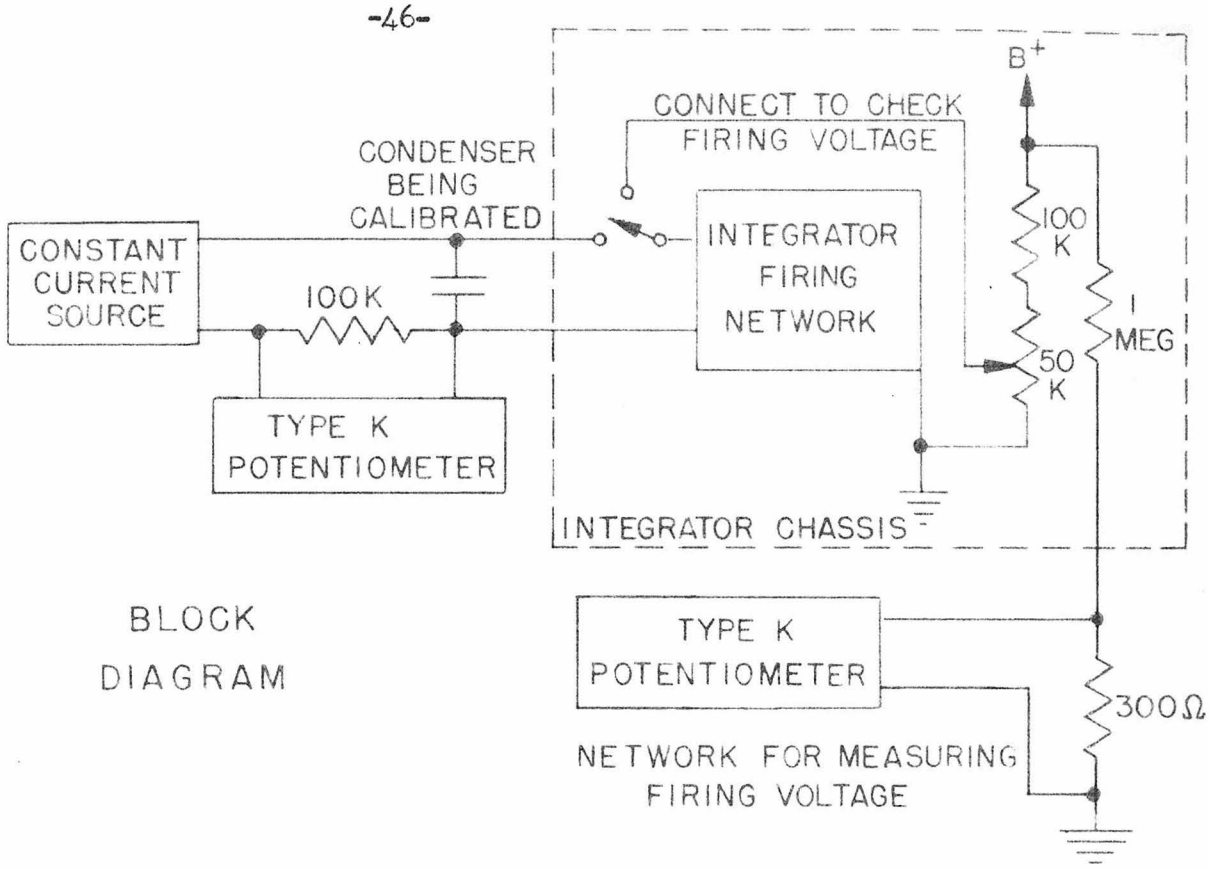

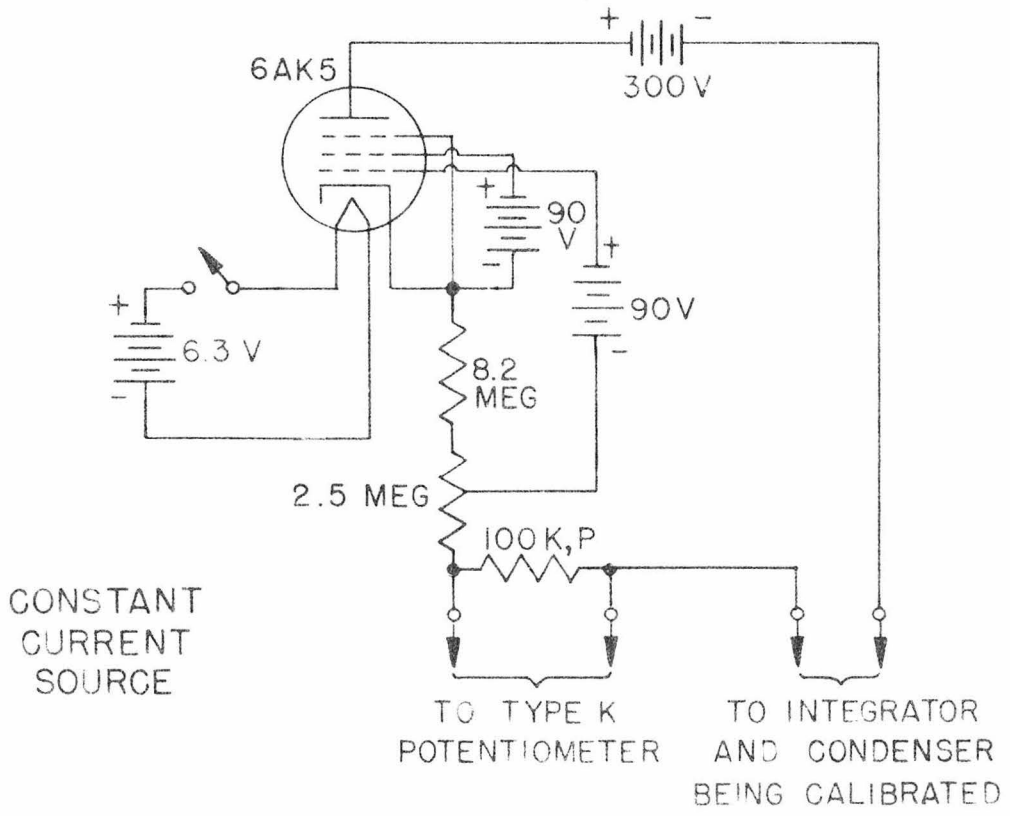

FIG. 11 INTEGRATOR CALIBRATION CIRCUIT

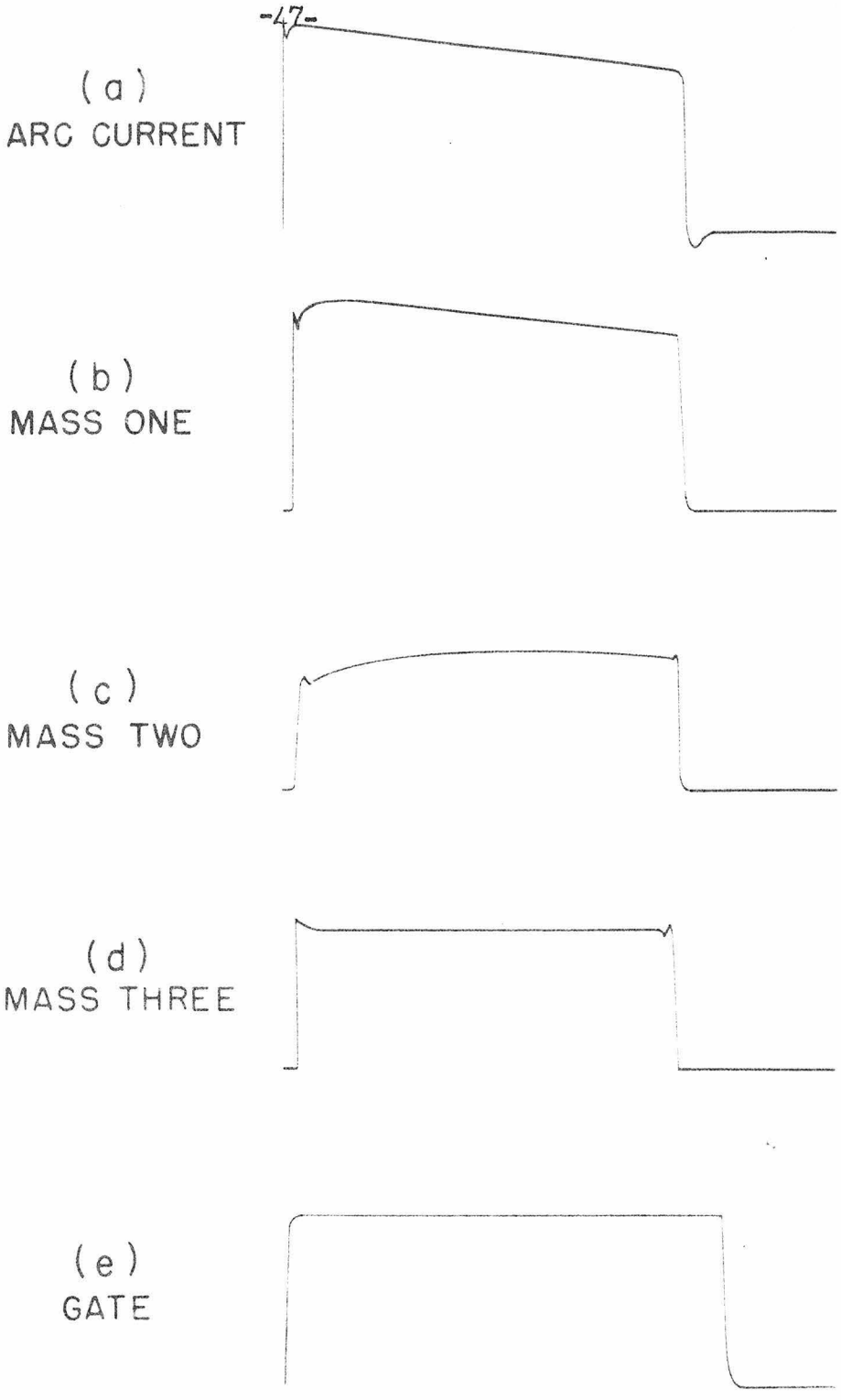

FIG. 12 WAVEFORMS OF MASS COMPONENT CURRENTS

SCALE: 1" = 250 MICROSECONDS

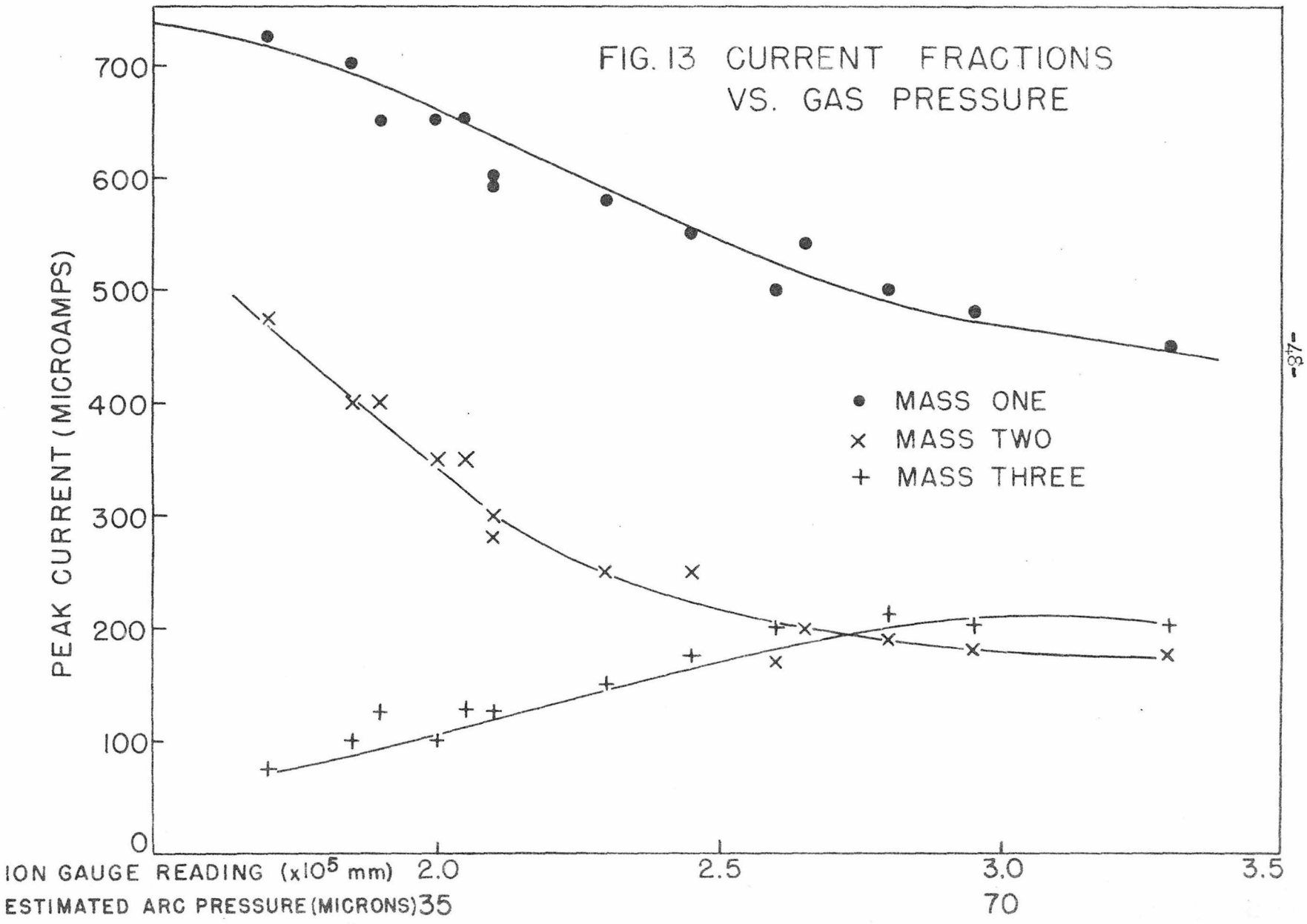
FIG. 13 CURRENT FRACTIONS
VS. GAS PRESSURE
PEAK CURRENT (MICROAMPS)
700
600
500
400
300
200
100
0
MASS ONE
MASS TWO
MASS THREE
ION GAUGE READING (x10⁵ mm) 2.0
2.5
3.0
3.5
ESTIMATED ARC PRESSURE (MICRONS) 35
70

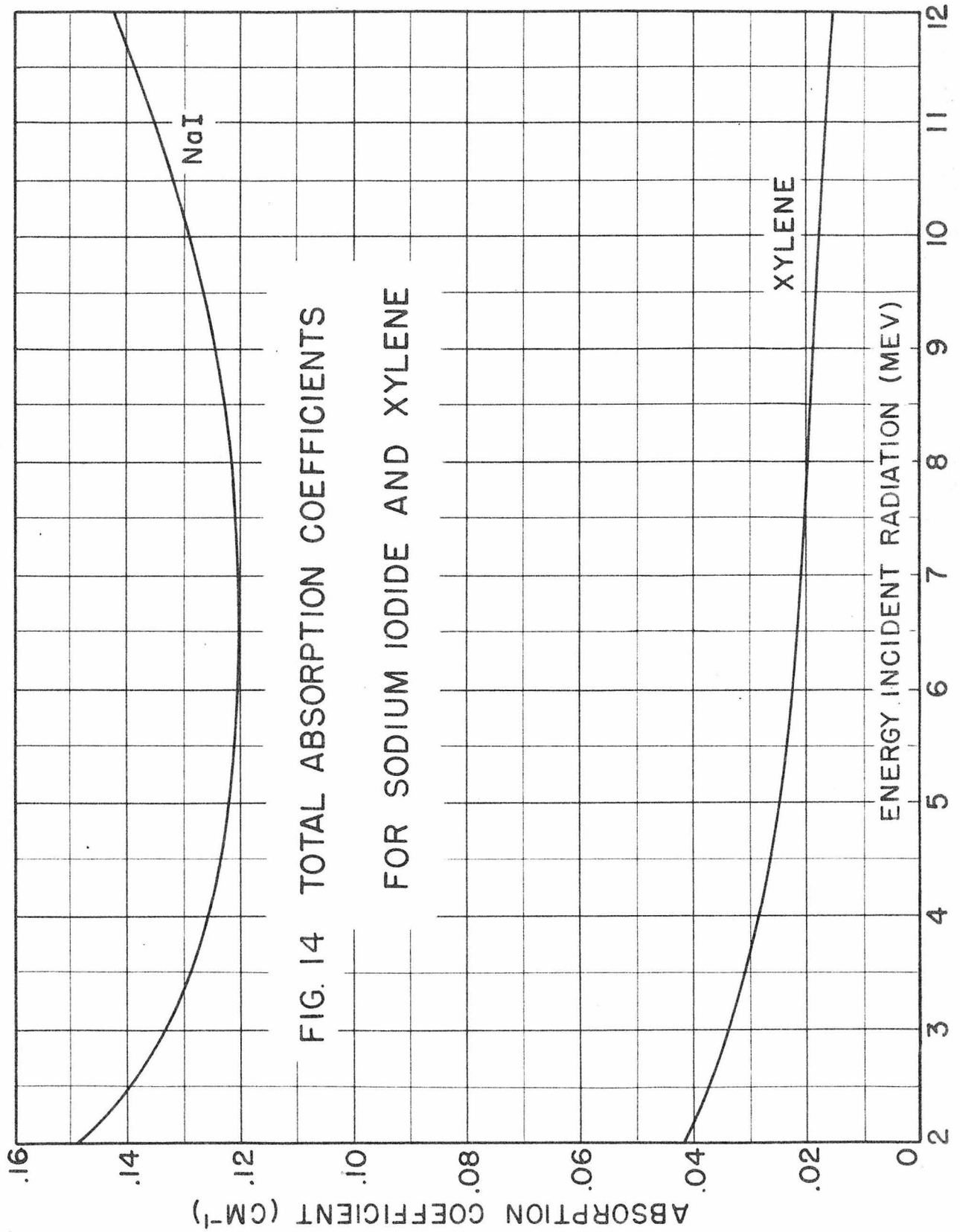

FIG. 14 TOTAL ABSORPTION COEFFICIENTS FOR SODIUM IODIDE AND XYLENE

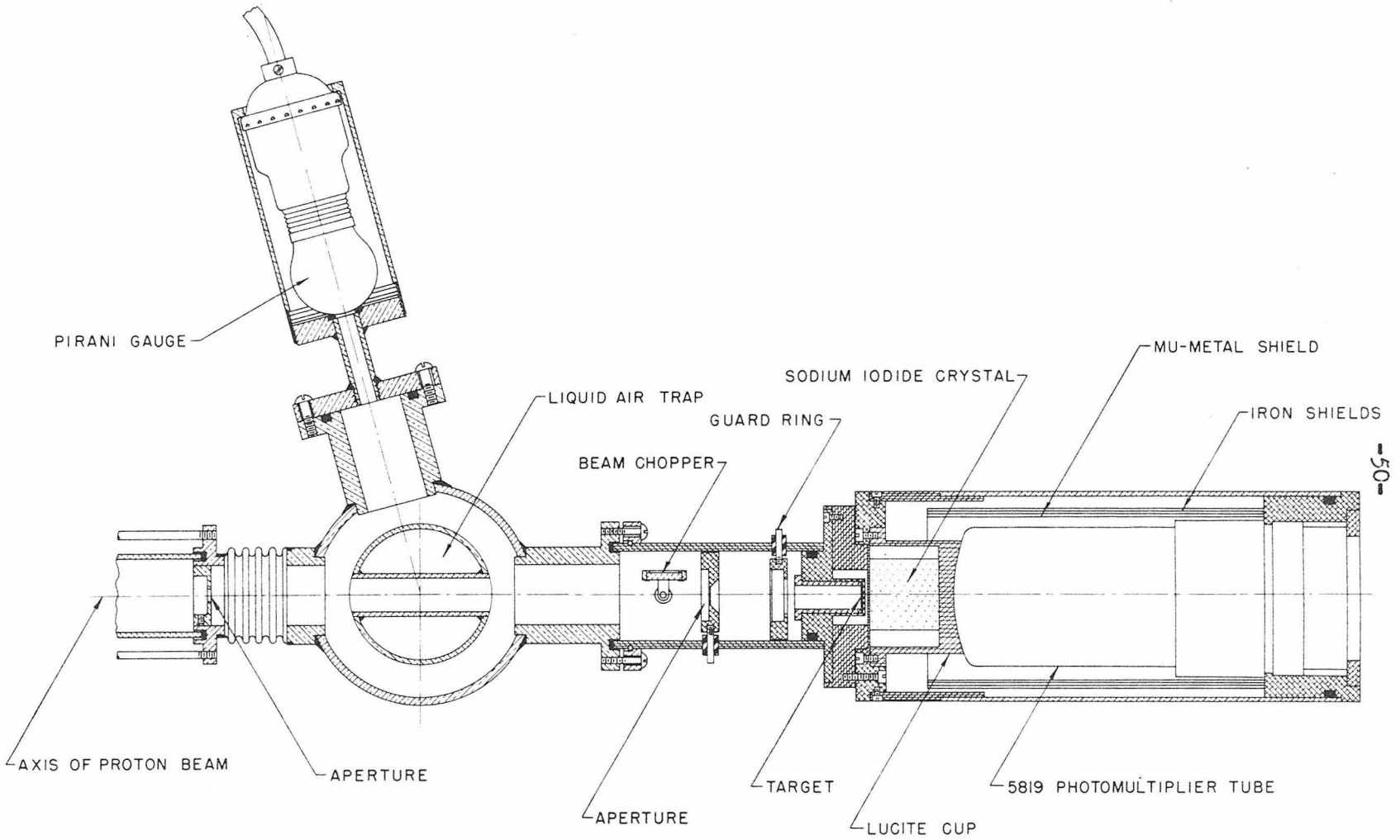

FIG. 15 TARGET CHAMBER AND COUNTER

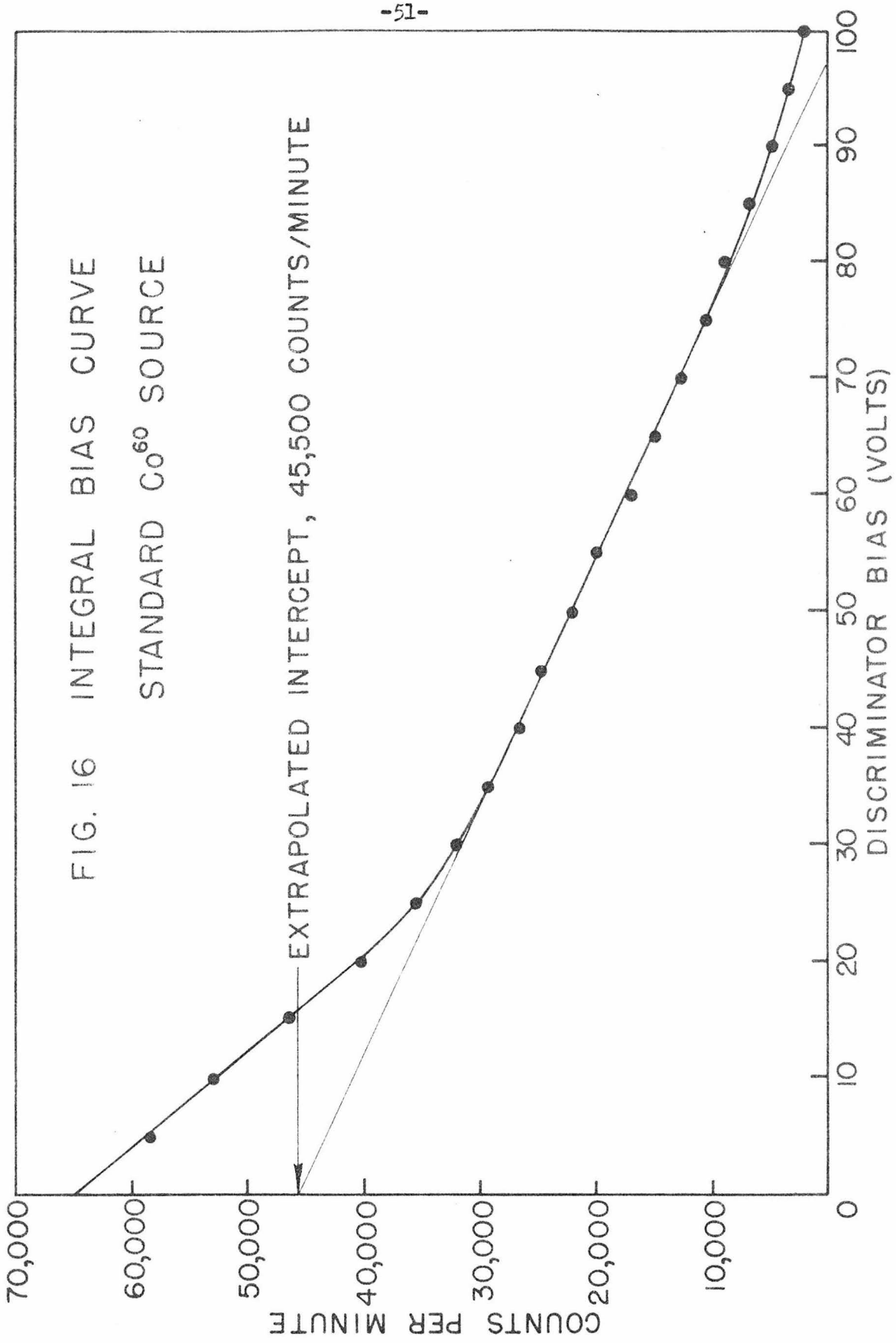
FIG. 16 INTEGRAL BIAS CURVE
STANDARD Co^{60} SOURCE
EXTRAPOLATED INTERCEPT, 45,500 COUNTS/MINUTE
COUNTS PER MINUTE
70,000
60,000
50,000
40,000
30,000
20,000
10,000
0
10
20
30
40
50
60
70
80
90
100
DISCRIMINATOR BIAS (VOLTS)

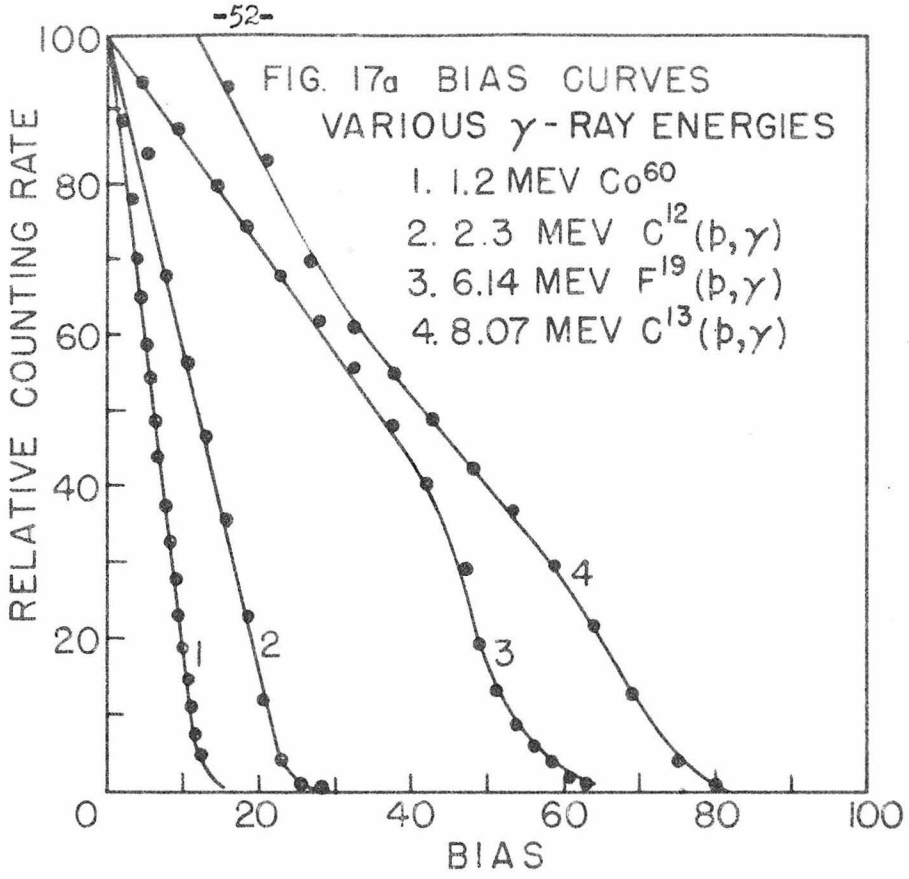
FIG. 17a BIAS CURVES
VARIOUS γ-RAY ENERGIES
1. 1.2 MEV Co60
2. 2.3 MEV C12(p,γ)
3. 6.14 MEV F19(p,γ)
4. 8.07 MEV C13(p,γ)
RELATIVE COUNTING RATE
BIAS
0
20
40
60
80
100
1
2
3
4

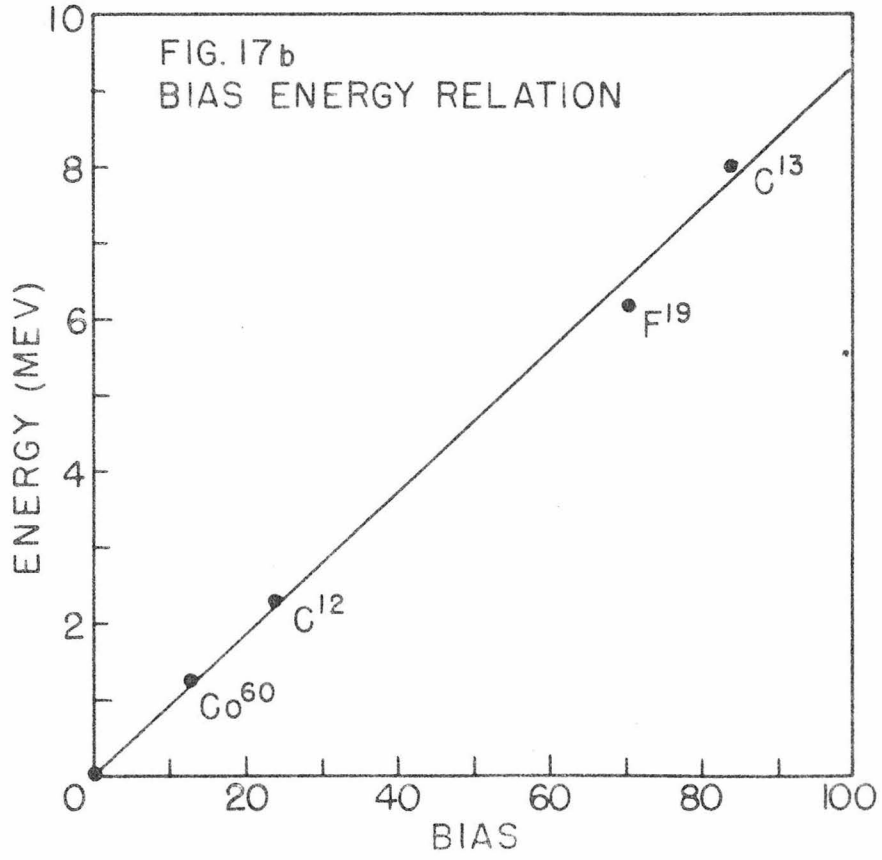
FIG. 17b
BIAS ENERGY RELATION
ENERGY (MEV)
BIAS
0
2
4
6
8
10
20
40
60
80
100
C13
F19
C12
Co60

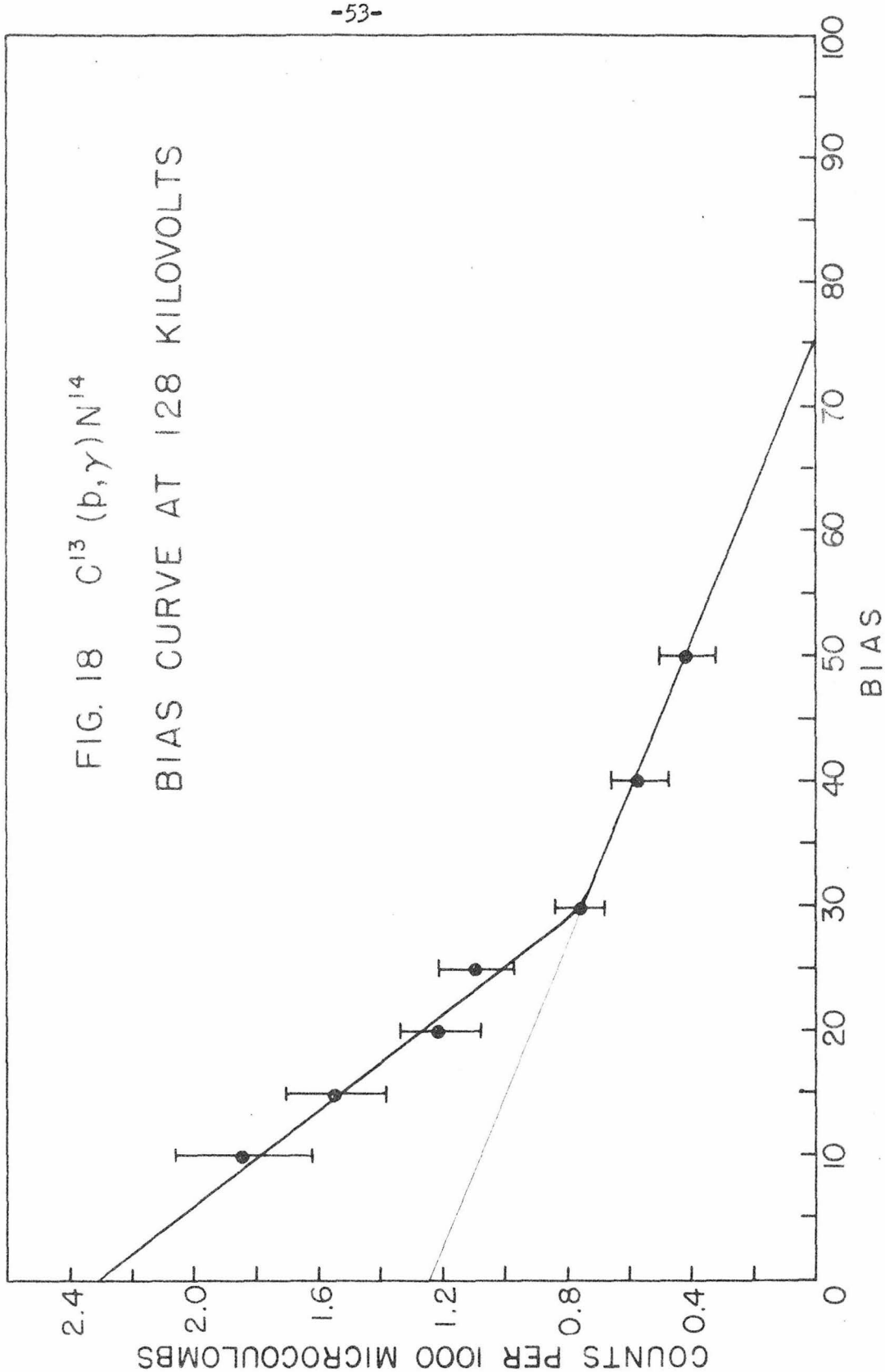
FIG. 18 $C^{13}(b,\gamma)N^{14}$
BIAS CURVE AT 128 KILOVOLTS
COUNTS PER 1000 MICROCOULOMBS
2.4
2.0
1.6
1.2
0.8
0.4
0
10
20
30
40
50
60
70
80
90
100
BIAS

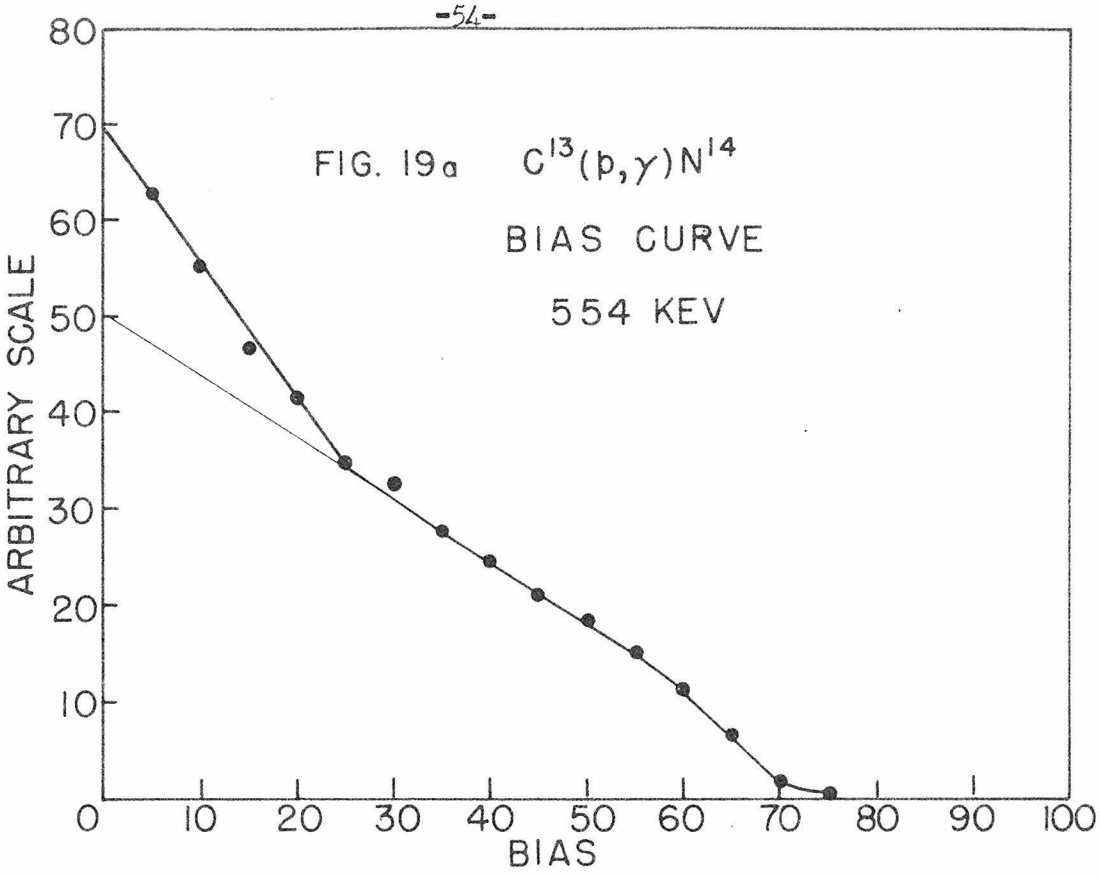
FIG. 19a $C^{13}(p,\gamma)N^{14}$
BIAS CURVE
554 KEV
ARBITRARY SCALE
BIAS
0
10
20
30
40
50
60
70
80
90
100

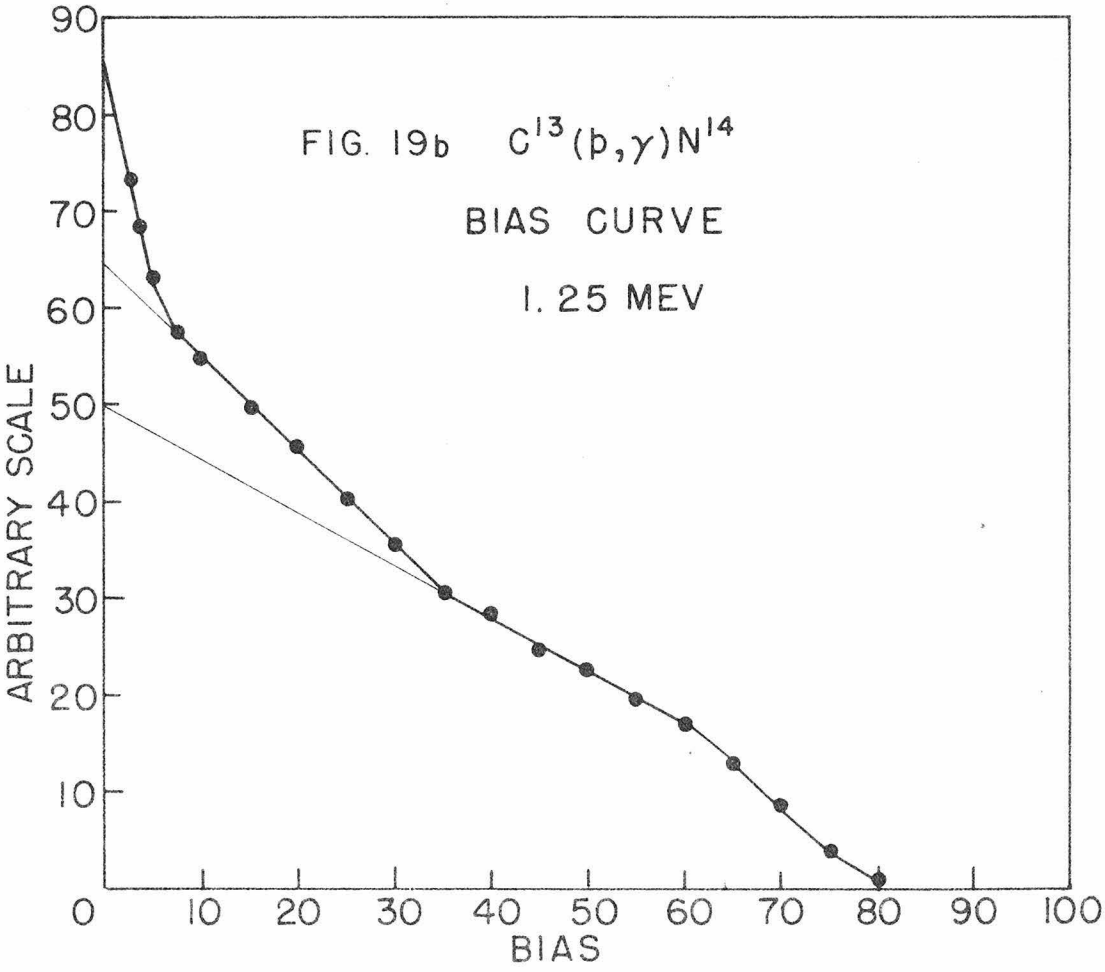
FIG. 19b $C^{13}(p,\gamma)N^{14}$
BIAS CURVE
1.25 MEV
ARBITRARY SCALE
BIAS
0
10
20
30
40
50
60
70
80
90
100

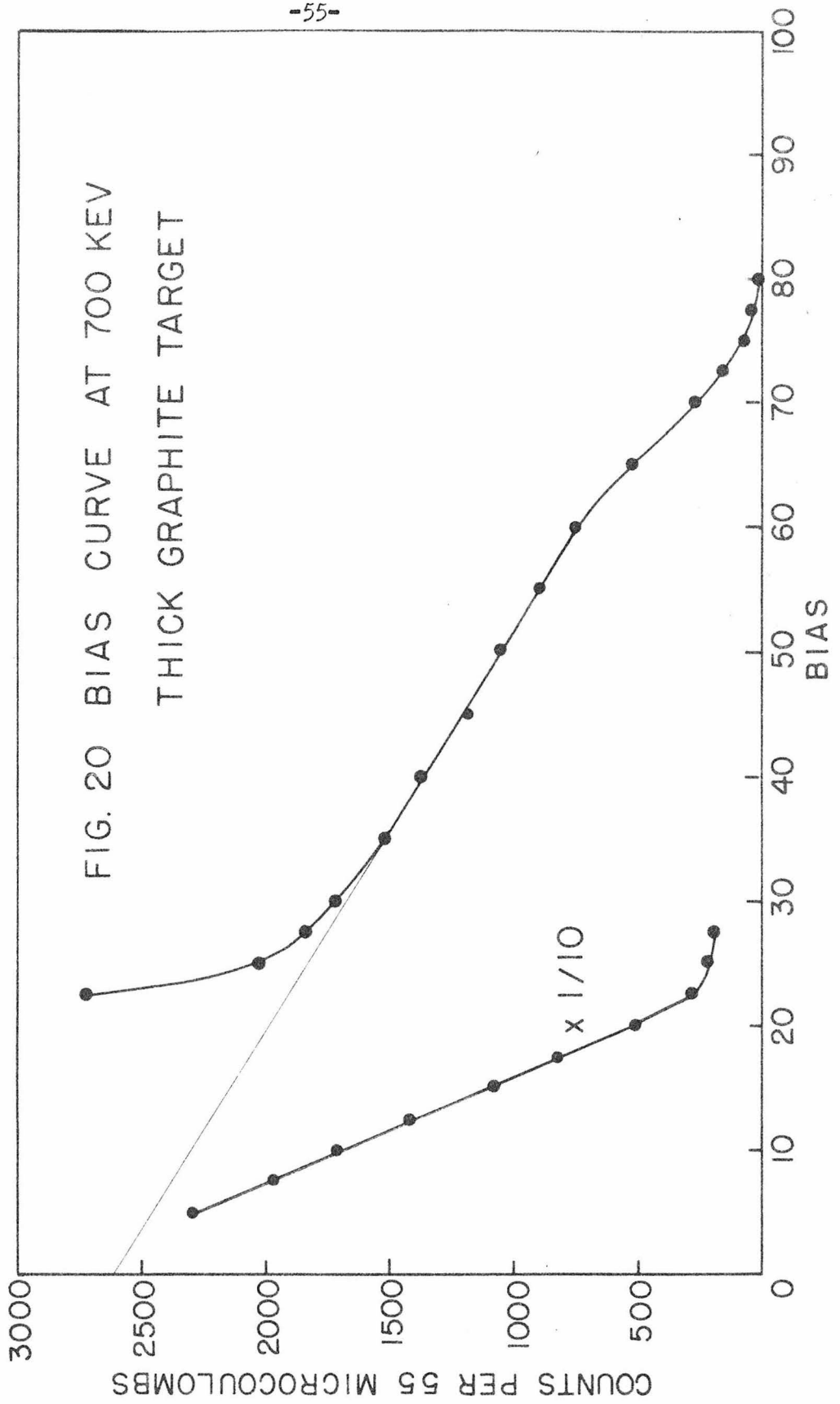
FIG. 20 BIAS CURVE AT 700 KEV
THICK GRAPHITE TARGET
x 1/10
COUNTS PER 55 MICROCOULOMBS
3000
2500
2000
1500
1000
500
0
10
20
30
40
50
60
70
80
90
100
BIAS

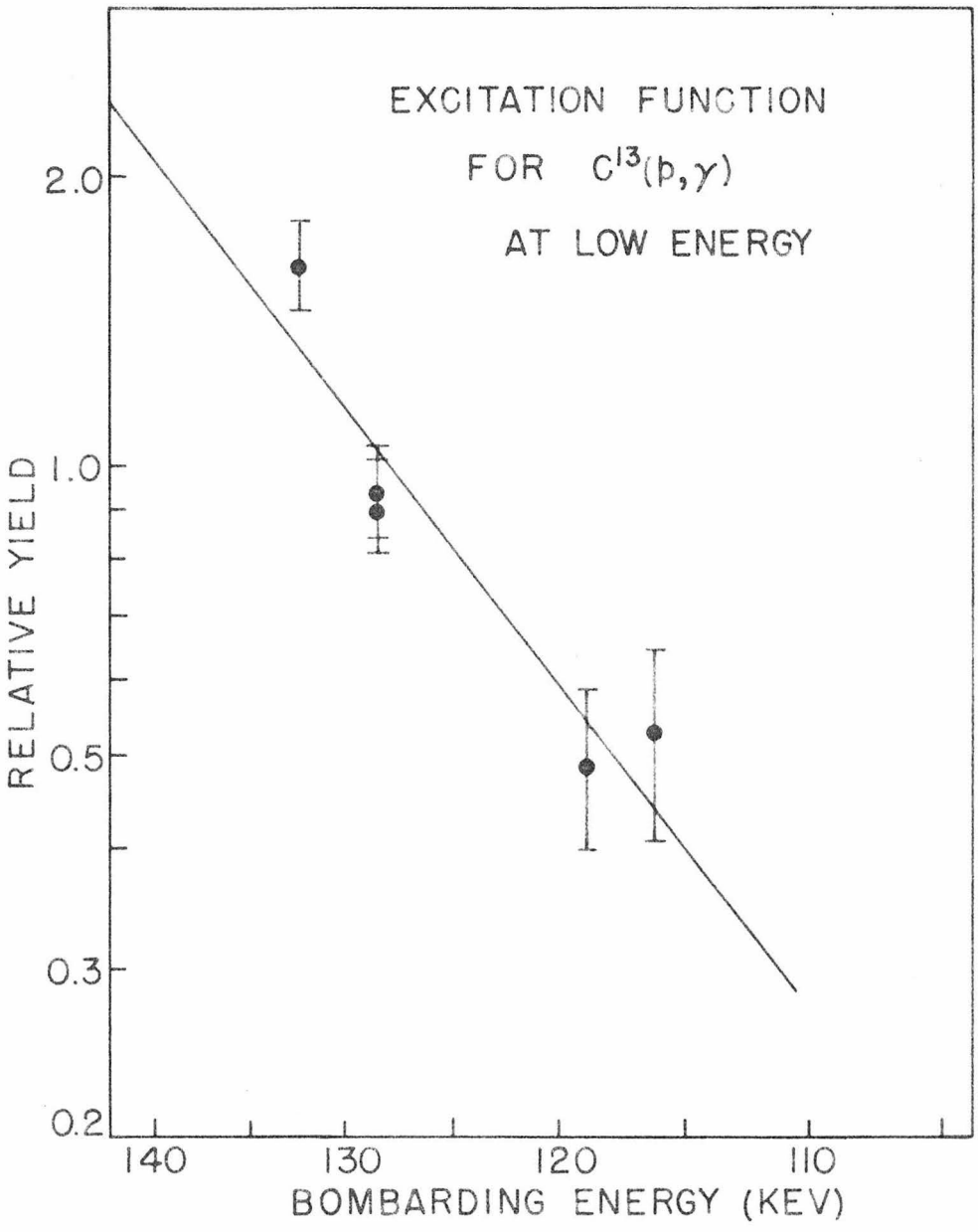
EXCITATION FUNCTION
FOR $C^{13}(p,\gamma)$
AT LOW ENERGY
RELATIVE YIELD
2.0
1.0
0.5
0.3
0.2
140
130
120
110
BOMBARDING ENERGY (KEV)

FIG. 21